# Electron and nuclear dynamics of molecular clusters in ultraintense laser fields. III. Coulomb explosion of deuterium clusters

Isidore Last and Joshua Jortner[a)]
*School of Chemistry, Tel Aviv University, Ramat Aviv, 69978 Tel Aviv, Israel*

(Received 25 March 2004; accepted 21 May 2004)

In this paper we present a theoretical and computational study of the energetics and temporal dynamics of Coulomb explosion of molecular clusters of deuterium $(D_2)_{n/2}$ ($n=480-7.6\times10^4$, cluster radius $R_0=13.1-70$ Å) in ultraintense laser fields (laser peak intensity $I=10^{15}-10^{20}$ W cm$^{-2}$). The energetics of Coulomb explosion was inferred from the dependence of the maximal energy $E_M$ and the average energy $E_{av}$ of the product $D^+$ ions on the laser intensity, the laser pulse shape, the cluster radius, and the laser frequency. Electron dynamics of outer cluster ionization and nuclear dynamics of Coulomb explosion were investigated by molecular dynamics simulations. Several distinct laser pulse shape envelopes, involving a rectangular field, a Gaussian field, and a truncated Gaussian field, were employed to determine the validity range of the cluster vertical ionization (CVI) approximation. The CVI predicts that $E_{av}$, $E_M \propto R_0^2$ and that the energy distribution is $P(E)\propto E^{1/2}$. For a rectangular laser pulse the CVI conditions are satisfied when complete outer ionization is obtained, with the outer ionization time $t_{oi}$ being shorter than both the pulse width and the cluster radius doubling time $\tau_2$. By increasing $t_{oi}$, due to the increase of $R_0$ or the decrease of $I$, we have shown that the deviation of $E_{av}$ from the corresponding CVI value ($E_{av}^{CVI}$) is $(E_{av}^{CVI}-E_{av})/E_{av}^{CVI}\simeq(t_{oi}/2.91\tau_2)^2$. The Gaussian pulses trigger outer ionization induced by adiabatic following of the laser field and of the cluster size, providing a pseudo-CVI behavior at sufficiently large laser fields. The energetics manifest the existence of a finite range of CVI size dependence, with the validity range for the applicability of the CVI being $R_0 \leqslant (R_0)_I$, with $(R_0)_I$ representing an intensity dependent boundary radius. Relating electron dynamics of outer ionization to nuclear dynamics for Coulomb explosion induced by a Gaussian pulse, the boundary radius $(R_0)_I$ and the corresponding ion average energy $(E_{av})_I$ were inferred from simulations and described in terms of an electrostatic model. Two independent estimates of $(R_0)_I$, which involve the cluster size where the CVI relation breaks down and the cluster size for the attainment of complete outer ionization, are in good agreement with each other, as well as with the electrostatic model for cluster barrier suppression. The relation $(E_{av})_I \propto (R_0)_I^2$ provides the validity range of the pseudo-CVI domain for the cluster sizes and laser intensities, where the energetics of $D^+$ ions produced by Coulomb explosion of $(D)_n$ clusters is optimized. The currently available experimental data [Madison *et al.*, Phys. Plasmas **11**, 1 (2004)] for the energetics of Coulomb explosion of $(D)_n$ clusters ($E_{av}=5-7$ keV at $I=2\times10^{18}$ W cm$^{-2}$), together with our simulation data, lead to the estimates of $R_0=51-60$ Å, which exceed the experimental estimate of $R_0=45$ Å. The predicted anisotropy of the $D^+$ ion energies in the Coulomb explosion at $I=10^{18}$ W cm$^{-2}$ is in accord with experiment. We also explored the laser frequency dependence of the energetics of Coulomb explosion in the range $\nu=0.1-2.1$ fs$^{-1}$ ($\lambda=3000-140$ nm), which can be rationalized in terms of the electrostatic model. © *2004 American Institute of Physics.* [DOI: 10.1063/1.1772366]

## I. INTRODUCTION

Features of light-matter interactions emerge from the interaction of clusters with ultrashort (pulse temporal length $\tau=10-100$ fs) and ultraintense (peak intensity $I=10^{15}-10^{20}$ W cm$^{-2}$) laser fields. While the coupling of macroscopic dense matter, e.g., liquids and solids with ultraintense laser fields, is blurred by inhomogeneous dense plasma formation, isochoric heating, beam self-focusing, and radiative continuum production effects,[1–3] the response of large molecules or clusters (whose size is considerably smaller than the laser wavelength) with ultraintense laser fields trigger well-characterized ultrafast dynamics of electrons (on the time scale of ~1–50 fs), of nuclei or of highly charged ions (on the time scale of 10–100 fs) in these large finite systems.[4–37]

On the basis of our recent analyses and simulations,[36,37] the electron dynamics of clusters in ultraintense laser fields involves three sequential-parallel coupled processes of inner ionization, which results in the formation of a charged, energetic nanoplasma within the cluster (or its vicinity), and in the (partial or complete) outer ionization of the nanoplasma. The yields and time-resolved dynamics of these three coupled electronic processes, which depend on the laser intensity and pulse shape, the cluster size, and the elec-

a)Electronic mail: jortner@chemsgl.tau.ac.il

 

tronic level structure of the constituents, were recently explored.[36,37] The electron dynamic processes trigger nuclear dynamics, with the outer ionization being accompanied by cluster Coulomb explosion, which results in the production of highly energetic (keV-MeV) multicharged ions on the ultrashort (10–100 fs) time scale.[6,17,18,28,34] When the time scales for both inner ionization and outer ionization electronic processes are considerably faster than the nuclear process of Coulomb explosion, the cluster vertical ionization (CVI) approximation becomes valid.[28,36,37] The CVI approximation, which implies that at the temporal onset of Coulomb explosion the inner and the outer ionizations are already completed, decouples the dynamics of heavy particles (ions) from the dynamics of electrons. When the CVI conditions are realized, Coulomb explosion of the highly charged ionic cluster, which is stripped of all the nanoplasma electrons, involves a nuclear dynamic process, which was previously addressed.[38–41] The spatially isotropic (or nearly so) cluster Coulomb explosion (resulting in individual ions), which reflects on the instability of multicharged systems, is realized for the Rayleigh fissibility parameter, $X=$(Coulomb energy/2 surface energy), being $X>1$, while for $X<1$ cluster fission into large ionic fragments is manifested.[38,39]

An important outcome of cluster Coulomb explosion of multicharged clusters is the production of energetic (keV-MeV) ions. The energetics of the ions produced by Coulomb explosion is of particular interest in the case of deuterium or/and tritium containing clusters when Coulomb explosion in an assembly of multicharged ionic clusters drives nuclear fusion.[25–28,30,33] The kinetic energy of the ions can be estimated by classical dynamics simulations of the motion of cluster energetic electrons and ions.[27,28,32] The treatment of this problem is highly simplified, sometimes even being reduced to the analytic algebraic equations for the ion energy, when the CVI conditions are fulfilled and the kinetic energy of the ions is determined by the ion-ion Coulomb interactions.[25,28,32,40,41] The kinetic energy of ions for the CVI conditions for a fixed ionization level does not depend on laser intensity I if one ignores the direct effect of the laser field on the ions, which is small even at very high laser intensities of $I\sim 10^{18}-10^{19}\,\mathrm{W\,cm^{-2}}$. The decrease of the laser intensity to a cluster size dependent lower intensity domain $I$ (of $I\lesssim 10^{17}\,\mathrm{W\,cm^{-2}}$ for moderately large clusters with $R\lesssim 50$ Å) results in the violation of the CVI conditions and in the decrease of the kinetic energy of the ions.[28] In this laser intensity domain the energetics of the ions has to be determined by dynamic simulations, which treat not only the ions but also the electrons. Our recent papers on extreme multielectron ionization and electron dynamics in molecular clusters in ultraintense laser fields[36,37] (referred to as Papers I and II, respectively) provide the basis for the study of nuclear dynamics of Coulomb explosion. In the present paper (Paper III of the series) this is explored for deuterium clusters and in the subsequent paper[42] (Paper IV of this series) for elemental clusters consisting of heavy many-electron atoms and of deuterium containing heteroclusters.

In this paper we study Coulomb explosion in molecular clusters of deuterium $(D_2)_{n/2}$ $(n=480-7.6\times 10^4)$ clusters in ultraintense $(I=10^{15}-10^{20}\,\mathrm{W\,cm^{-2}})$ laser fields, using classical dynamics simulations.[17,28,36,37] Several distinct pulse shape envelopes, involving a Gaussian laser field,[43–45] a rectangular laser field, and a truncated Gaussian laser field,[23] were employed. From the point of view of methodology, we shall determine the validity domain for the CVI approximations[40,41] for the cluster inner/outer ionization. Subsequently, we shall study the nuclear energetics of Coulomb explosion, which occurs in parallel and sequentially with outer ionization. In this context we report results for the dependence of the energetics of Coulomb explosion on the pulse shape, the pulse intensity, the pulse temporal duration, and the frequency of the ultraintense laser. These data will reflect on the dynamics of the coupled electron-nuclear-laser system, and are of interest in the context of the control of Coulomb explosion processes by the shaping of the laser pulse.[45–47]

An interesting development involves dd nuclear fusion driven by Coulomb explosion (NFDCE) of deuterium containing homonuclear $(D_2)_{n/2}$ clusters [labeled as $(D)_n$], and heteronuclear $(D_2O)_n$ and $(CD_4)_n$ clusters, for which compelling experimental[25,26,30,33] and theoretical[27,28,32] evidence became available. In this context, the exploration of Coulomb explosion of neat deuterium clusters will be of intrinsic interest for the elucidation of the benchmark results for the dynamics of NFDCE.

## II. CLUSTER VERTICAL IONIZATION

In order to utilize approximate analytic expressions for the energetics and the temporal dynamics of Coulomb explosion, we advance the CVI approximation[40,41] for cluster ionization, together with its energetic and dynamic implications, which will be confronted with simulation results. The multielectron ionization of clusters is vertical when inner ionization and complete outer ionization occur at a fixed cluster atomic geometry of the neutral ground state. Vertical cluster ionization is realized provided that the following conditions are simultaneously satisfied:

(i) Separation of time scales between the electronic (''short'') inner/outer ionization and the (''long'') nuclear process of Coulomb explosion.

(ii) The outer ionization process is complete on the ''short'' time scale for electron dynamics.

In the case of CVI, the subsequent Coulomb explosion is described as a spatial expansion of ions with fixed charges (in the absence of the nanoplasma). This limiting description significantly simplifies the treatment of the Coulomb explosion process. The dynamics and energetics of Coulomb explosion can be described by analytical expressions, provided that: (1) the CVI conditions are fulfilled and (2) the ion density, charge, and mass are initially uniform. We shall show that these exploding clusters retain their uniform distribution during their spatial expansion. The simplest case of uniformly expanding clusters corresponds to homonuclear deuterium clusters, which we describe as $(D^+)_n$ clusters of ionized one-electron $D^+$ atoms of mass $m$ and charge $q=1$. The dynamics of the ion expansion of the uniformly expanding

homonuclear clusters was previously addressed[28,32] and will be presented and analyzed in detail. The uniform Coulomb explosion time $t$ of an ion is given by

$$t = Cq^{-1}(m/\rho)^{1/2}Z(\xi), \tag{1}$$

where

$$\xi = r_0/r(t), \tag{2a}$$

$$Z(\xi) = \frac{(1-\xi)^{1/2}}{\xi} + \frac{1}{2}\ln\left(\frac{1+(1-\xi)^{1/2}}{1-(1-\xi)^{1/2}}\right). \tag{2b}$$

Here $r_0$ is the initial distance of the ion from the cluster center, $r(t)$ is the distance of this ion from the center at time $t$, $\rho$ is the initial molecular ion density $\rho = (4\pi r_a^3 f/3)^{-1}$, with $r_a$ being the constituent radius and $f$ being the packing fraction within the neutral cluster. The following units will be used herein: the mass of a constituent atom $m$ in amu, the constituent charges $q$ in $e$, the distances in Å, the molecular density $\rho$ in $\text{Å}^{-3}$, and $t$ in fs. The coefficient $C$ of Eq. (1) is then $C = 0.931\ \text{fs Å}^{-3/2}$. Each ion initially located at $r_0$ moves to $r(t;r_0)$ at time $t$. As, according to Eq. (2a), $r(t;r_0) = r_0\xi(t)^{-1}$, the cluster radial expansion is uniform. The Coulomb explosion time $t(\xi^{-1})$ for the expansion of the cluster radius from its initial value of $R_0$ by a numerical factor of $\xi^{-1}(>1)$, is given by Eq. (1). The time, $\tau_2 = t(2)$, for the cluster radius doubling [$\xi^{-1}=2$, $\xi=0.5$, $Z(\xi)=2.296$] is

$$\tau_2 = 2.137q^{-1}(m/\rho)^{1/2}. \tag{3}$$

The characteristic Coulomb explosion times $\tau_2$, Eq. (3), for uniformly exploding homonuclear clusters reveal the following features:

(1) Charge dependence. $\tau_2 \propto q^{-1}$, exhibiting a reciprocal dependence of the ion charges, in accord with previous analyses and simulations.[28,32]

(2) Mass effect, with $\tau_2 \propto (m)^{1/2}$. For Coulomb explosion of homonuclear clusters, e.g., $(H^+)_n$, $(D^+)_n$, and $(T^+)_n$, this result exhibits an isotope effect on the time scale of nuclear dynamics.

(3) Dependence on the neutral cluster structure, with $\tau_2 \propto (\rho)^{-1/2} \propto (r_a)^{3/2}$. This result reflects on the lengthening of $\tau_2$ for a larger size of the initial homonuclear cluster constituents.

(4) Cluster size independence. No cluster size dependence of $\tau_2$ is expected. The absence of size scaling is expected to prevail for sufficiently large clusters where the continuum approximation for the derivation of Eq. (1) holds. From numerical simulations of Coulomb explosion of $(Xe^{q+})_n$ clusters ($q=1\cdots8$) under CVI conditions,[40] we inferred that the size invariance of $\tau_2$ sets in for $n>35$. Accordingly, all our calculations and simulations for Coulomb explosion of multicharged molecular clusters were performed for sufficiently large clusters, with $n>55$. For sufficiently large $(D^+)_n$ clusters, $\tau_2 = 13.5$ fs.

We now turn to the energetics of ions from uniformly Coulomb exploding $(A^{q+})_n$ homonuclear clusters. On the basis of simple electrostatic arguments the kinetic energy $E[r(t)]$ of the $A^{q+}$ ion, which is located at the distance $r(t)$ from the cluster center at time $t$, is given by

$$E[r(t)] = (4\pi/3)B\rho q^2 r_0^2[1-\xi(t)], \tag{4}$$

where $B = 14.385\ \text{eV Å}$ and $\xi(t)$ is given by Eq. (2a). The final ($\xi\to0, r\to\infty$) kinetic energy $E$ is proportional to the square of its initial distance $r_0$ from the cluster center, whereupon

$$E(r_0) = (4\pi/3)B\rho q^2 r_0^2. \tag{5}$$

A numerical solution of Eq. (1) results in $r(t)$, which is substituted into Eq. (4) to find the time dependence of an ion kinetic energy and velocity. Making use of Eq. (5), the average energy $E_{\text{av}}$ and the maximal energy $E_{\text{M}}$ of the ions are given by

$$E_{\text{av}} = (4\pi/5)B\rho q^2 R_0^2, \tag{6}$$

$$E_{\text{M}} = (4\pi/3)B\rho q^2 R_0^2, \tag{7}$$

where $R_0$ is the initial cluster radius. The energy distribution $P(E_j)$ of the ions is

$$P(E) = \frac{3}{2}(E/E_M^3)^{1/2}. \tag{8}$$

From this analysis we infer the following for the energetics, Eqs. (6)–(8), of uniformly exploding clusters:

(1) Cluster size dependence. Both $E_{\text{M}}$ and $E_{\text{av}}$ scale as $R_0^2$. These relations constitute divergent cluster size equations, which do not converge to the response of the macroscopic system for $R_0\to\infty$. This is a unique feature in the context of cluster size equations.

(2) Relation between maximal and average energies. The simple relation $E_{\text{M}}/E_{\text{av}} = 5/3$ is applicable.

(3) Charge dependence. The relation $E_{\text{M}}$, $E_{\text{av}} \propto q^2$ is a consequence of the electrostatic energy in a multicharged cluster which underwent CVI.

(4) Ion mass dependence. The energies, as expressed by Eqs. (6) and (7), are independent of $m$, in contrast with the results for $\tau_2$, Eq. (3). For Coulomb explosion of homonuclear clusters, e.g., $(H^+)_n$, $(D^+)_n$, and $(T^+)_n$, the average energies are not expected to manifest an isotope effect.

(5) Dependence on initial cluster configuration. $E_{\text{M}}$, $E_{\text{av}} \propto \rho \propto r_a^{-3}$, reflecting on the decrease of the ion energies for a larger size of the cluster initial constituents.

The analytic results for Coulomb explosion lifetimes and energies, Eqs. (3) and (6)–(8), provide benchmark reference data, which can be used to define the domain of cluster size and laser parameters, where the CVI conditions for uniformly exploding clusters are applicable. When are the CVI and/or uniform explosion conditions violated? For uniformly exploding clusters, encompassing $(H_2^{2+})_{n/2}$ [also denoted as $(H^+)_n$], $(D_2^{2+})_{n/2}[\equiv(D^+)_n]$, and $(T_2^{2+})_{n/2}[\equiv(T^+)_n]$, the CVI approximation will break down at low laser intensities. Under these circumstances we expect inner/outer ionization processes to occur on a slower time scale than at the higher intensities (Paper II), with the outer ionization process being incomplete (on a time scale of ~50 fs) (Papers I and II). This results in screening effects of Coulomb repulsions by nanoplasma electrons, which retard the energetics of Coulomb explosion. These interesting effects of the violation of the CVI model will be explored by molecular dynamics simula-

tions of the energetic electron dynamics and of nuclear dynamics, using the computational schemes previously advanced by us (Paper I).

## III. EFFECTS OF LASER PULSE SHAPE AND WIDTH ON THE ENERGETICS AND DYNAMICS OF COULOMB EXPLOSION

The laser pulses used in the experiments[43–45] are mostly of Gaussian shape, and in our previous Papers I and II the cluster ionization processes were studied for such Gaussian shaped pulses. In the present work we will also mainly deal with the Gaussian shaped pulse. However, in order to establish how the pulse shape affects the ion energy, we performed some additional simulations using a rectangular pulse and a strongly truncated Gaussian shaped pulse.[17,23]

The laser electric field was taken as

$$F_\ell(t)=F_{\ell 0}(t)\cos(2\pi\nu t+\phi_0) \tag{9}$$

(for $-\infty<t<\infty$) with the frequency $\nu=0.35$ fs$^{-1}$ (photon energy 1.44 eV). All the results presented in Secs. III–VI for electron and nuclear dynamics were obtained from this laser frequency. In Sec. VII the treatment is extended to explore the laser frequency dependence. The laser phase is taken as $\phi_0=0$, and $F_{\ell 0}(t)$ in Eq. (9) is the laser field envelope. The Gaussian shaped envelope function of the pulse is

$$F_{\ell 0}(t)=F_{\mathrm{M}}\exp[-2.773(t/\tau)^2], \tag{10}$$

where $F_{\mathrm{M}}$ is the maximal electric field (which is related to the laser peak intensity by $|eF_{\mathrm{M}}|=2.75\times10^{-7}I^{1/2}$ eV Å$^{-1}$ when $I$ is given in W cm$^{-2}$), and $\tau$ (in fs) is the pulse temporal width. For simulations (Papers I and II) with the Gaussian pulse, Eq. (10), we have used a weakly truncated Gaussian shaped pulse whose initial laser field amplitude is $F_{\ell 0}(t_s)=F_s>0$ and whose initial time $t_s<0$ has to be specified. In Paper I we determined the initial laser field as $F_s=(F^{\mathrm{th}}+F^{\mathrm{co}})/2$, where $F^{\mathrm{th}}$ is the threshold field for the first (single electron) ionization of each molecule, while $F^{\mathrm{co}}$ is the laser field for complete one-electron ionization of all the constituent atoms (typical $F_s$ values are presented in Table II of Paper I). The pulse, Eq. (10), which is weakly truncated according to the foregoing recipe, will be referred to as a Gaussian pulse. The initial laser field for the Gaussian pulse interacting with deuterium clusters, $eF_s=6.0$ eV Å$^{-1}$ (Table II of Paper I), results in complete inner ionization of $(D_2)_{n/2}$ clusters at $t=t_s$ for the laser intensity range of $I\geqslant10^{15}$ W cm$^{-2}$, used herein. As the inner ionization process is instantaneous for the Gaussian pulse, as well as for other pulse shapes, only outer ionization is relevant for electron dynamics in $(D)_n$ clusters, which affects the ion dynamics.

Two additional pulse shapes were utilized: First, we used a (strongly) truncated Gaussian pulse whose shape[23] is characterized by a Gaussian pulse, with $t_s=-\tau/2$ and $F_s=0.5F_{\mathrm{M}}$, so that $F_{\ell 0}(t)=0$; $t<t_s$, and $F_{\ell 0}(t)$ is given by Eq. (10) for $t>t_s$. Second, a rectangular pulse was used, being defined by the envelope function

$$\begin{aligned} &F_{\ell 0}(t)=F_{\mathrm{M}}; \quad -\tau/2\leqslant t\leqslant\tau/2 \\ &F_{\ell 0}(t)=0; \quad t<-\tau/2 \quad \text{and} \quad t>\tau/2. \end{aligned} \tag{11}$$

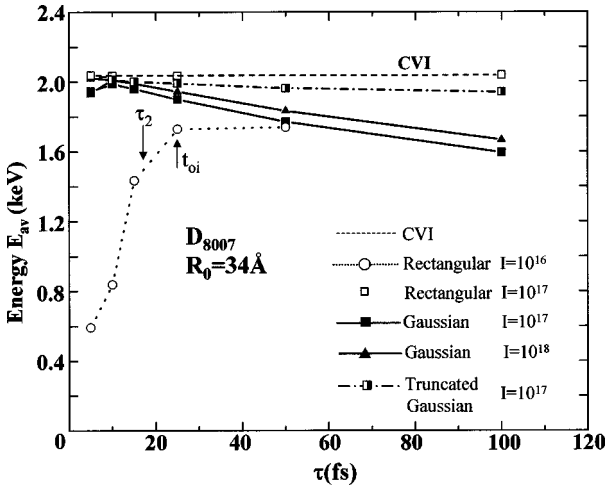


FIG. 1. The dependence of the average energy of $D^+$ ions from Coulomb explosion of $(D)_{8007}$ clusters induced by rectangular, Gaussian, and truncated Gaussian laser pulses with pulse widths $\tau$=5–100 fs and peak intensities $I=10^{16}$–$10^{18}$ W cm$^{-2}$. The characteristic times for complete outer ionization $(t_{\mathrm{oi}})_s$ and for the cluster doubling $\tau_2$ are marked on the curve for the rectangular pulse at $I=10^{16}$ W cm$^{-2}$. The CVI energy $E_{\mathrm{av}}=2.04$ eV, from Eq. (6), is also marked by a dashed line.

The electron and nuclear dynamics of the clusters subjected to the Gaussian, the truncated Gaussian, and the rectangular pulses were treated by the simulation methods previously described by us (Paper I), with the central output information being the ion energies, as well as electron dynamics, i.e., time scales for outer ionization, and ion dynamics, i.e., time scales for Coulomb explosion.

Simulations were performed for electron dynamics and Coulomb explosion energetics and dynamics of homonuclear $(D)_n$ clusters. In view of the complete inner ionization of the deuterium clusters in the laser intensity domain used herein (see above), we represented the molecular structure of $(A_2)_{n/2}$ clusters ($A$=H,$D$,T) in terms of a uniform initial distribution of $A$ atoms $[(A_2)_{n/2}\equiv(A)_n]$, which is characterized by the atomic density of liquid deuterium, $\rho=0.05$ Å$^{-3}$.[28] Figure 1 provides information on the pulse shape, width, and intensity dependence of the energetics of Coulomb explosion of $D_{8007}$ clusters, where we portray the dependence of the average $D^+$ ion energies $E_{\mathrm{av}}$ on the pulse width $\tau$ (in the range $\tau$=5–100 fs) for rectangular and Gaussian shaped pulses (in the intensity domain $I=10^{16}$–$10^{18}$ W cm$^{-2}$). The CVI energy $E_{\mathrm{av}}=2.04$ keV, calculated from Eq. (6), is also included in Fig. 1. This CVI energy is in good agreement with the energy $E_{\mathrm{av}}=2.03$ keV, obtained from molecular dynamics simulations of Coulomb explosion of a $(D^+)_{8007}$ cluster for the rectangular pulse at the higher intensity of $I=10^{17}$ W cm$^{-1}$.

The effect of the rectangular pulse width at the (lower) intensity domain of $I=10^{16}$ W cm$^{-2}$ (Fig. 1) reflects on the interplay between electron and nuclear dynamics in determining the ion energies. At $I=10^{16}$ W cm$^{-2}$ (Fig. 1), the energy of the ions generated by a rectangular pulse, Eq. (11), markedly increases by a numerical factor of 3.5 with increasing the pulse width in the range $\tau$=5 fs to $\tau$=25 fs, and subsequently reaches a saturation value for $\tau$=25–50 fs. This dependence of the ion energy on the rectangular pulse width

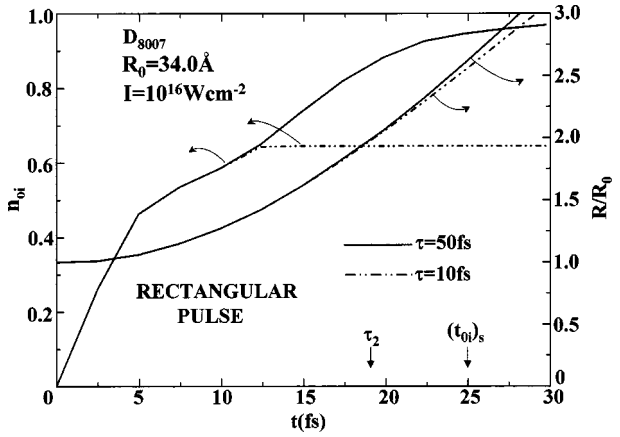


FIG. 2. Electron dynamics for outer ionization of $(D)_{8007}$ clusters, represented in the time dependence of the outer ionization level per atom, $n_{oi}$ for a rectangular pulse, at $I=10^{16}\,\mathrm{W\,cm^{-2}}$. For a pulse width of $\tau=50$ fs complete outer ionization occurs at $(t_{oi})_s=25$ fs, which is marked on the time scale, while for $\tau=10$ fs the saturation of incomplete outer ionization occurs at $t_{oi}\simeq 11$ fs$<(t_{oi})_s$, with $n_{oi}(t_{oi})\simeq 0.6$. Coulomb explosion dynamics, expressed by the time dependence of $R(t)/R_0$, is also presented for the two pulse widths, with the cluster radius doubling time $\tau_2$ being marked on the time scale.

at $I=10^{16}\,\mathrm{W\,cm^{-2}}$ can be rationalized on the basis of simulations of electron dynamics for outer ionization induced by a relatively long $\tau=50$ fs pulse (Fig. 2). For the subsequent discussion it will be convenient to define the time scale with the onset of the rectangular pulse at $t=0$. For the rectangular pulse we shall define the outer ionization time $t_{oi}$, when $n_{oi}(t>t_{oi})\simeq n_{oi}(t_{oi})$, for both complete $[n_{oi}(t_{oi})\simeq 1]$ and incomplete $[n_{oi}(t_{oi})<1]$ outer ionization, where $n_{oi}$ is the number of outer ionized electrons per atom. In general, $t_{oi}$ depends on the pulse intensity, the pulse duration, and the cluster size. When complete outer ionization is achieved during the rectangular laser pulse at the time $(t_{oi})_s$ (defined in Chap. II of Paper II as the time required for the attainment of 95% of the saturation level of the outer ionization), $(t_{oi})_s$ provides a good approximation of the time scale for complete outer ionization. In the time domain $t>(t_{oi})_s$ the cluster outer ionization process is complete, so that the laser-ionized cluster interaction does not affect the ion energy. The parameter $(t_{oi})_s$ is intensity dependent and also manifests cluster size dependence. The simulation of the electron dynamics in $(D)_{8007}$ at $I=10^{16}\,\mathrm{W\,cm^{-2}}$ and $\tau=50$ fs (Fig. 2) shows that $(t_{oi})_s=25$ fs. We expect that for the pulse lengths of $\tau>(t_{oi})_s\simeq 25$ fs at $I=10^{16}\,\mathrm{W\,cm^{-2}}$, the ion energy from $(D)_{8007}$ becomes independent of the pulse width, in accord with the simulations of Fig. 1. On the other hand, when $\tau<(t_{oi})_s$, the outer ionization process is incomplete, and is terminated at the end of the pulse, as demonstrated in Fig. 2 for $\tau=10$ fs, where the outer ionization time ($t_{oi}\simeq 12$ fs) becomes nearly equal to the pulse width. From the foregoing analysis we infer the existence of two temporal domains for outer ionization induced by a rectangular pulse

$$\text{Region (I):}\quad t_{oi}=\tau;\qquad \tau<(t_{oi})_s, \tag{12a}$$

$$\text{Region (II):}\quad t_{oi}=(t_{oi})_s;\quad \tau>(t_{oi})_s. \tag{12b}$$

In Region (I) of the incomplete outer ionization, Eq. (12a), the early termination of the outer ionization process leaves a substantial population of electrons inside the cluster in the time domain $t>\tau$ after the termination of the pulse, as is the case for $(D)_{8007}$ at $I=10^{16}\,\mathrm{W\,cm^{-2}}$ and $\tau=10$ fs (Fig. 2). This persistence of the electron population of the nanoplasma at the intensity of $I=10^{16}\,\mathrm{W\,cm^{-2}}$ enhances the screening of the ion-ion Coulomb interactions, and results in the decrease of the ion energy with decreasing the pulse width, as manifested by the simulation results (Fig. 1). The saturation of the $E_{av}$ versus $\tau$ dependence occurs in Region (II) of complete outer ionization, Eq. (12b). Indeed, the saturation of $E_{av}$ versus $\tau$ at $I=10^{16}\,\mathrm{W\,cm^{-2}}$ is manifested when $\tau\gtrsim(t_{oi})_s$ (Fig. 1). Whether the CVI prevails in this case is determined by relative magnitudes of the outer ionization time $t_{oi}$ and the time scale for Coulomb explosion, which is characterized by the cluster radius doubling time $\tau_2$, Eq. (3). When $\tau_2<t_{oi}$, deviations from the CVI are manifested, even when saturation of $E_{av}$ versus $\tau$ is exhibited. Indeed, for the case of $D_{8007}$ at $I=10^{16}\,\mathrm{W\,cm^{-2}}$ the saturation energy level is lower by about 20% than the CVI energy (Fig. 1). Such a deviation from the CVI energy is due to the long complete outer ionization time $(t_{oi})_s=25$ fs (for $\tau=25$–$50$ fs), which is longer than $\tau_2=13.5$ fs estimated from Eq. (3). Accordingly, $\tau_2<t_{oi}$ (Fig. 1), whereupon the outer ionization process occurs in parallel with Coulomb explosion (Fig. 2), violating the CVI conditions.

The increase of the laser intensity to $I=10^{17}\,\mathrm{W\,cm^{-2}}$ for a rectangular pulse (for $\tau=5$–$50$ fs) drastically decreases the complete outer ionization time for a $(D)_{8007}$ cluster to $(t_{oi})_s=2.5$ fs. This time scale is lower than the minimal pulse width of $\tau=5$ fs used herein, so that $t_{oi}=(t_{oi})_s<\tau$ and all the data of Fig. 1 for this intensity correspond to Range (II) of complete outer ionization, with $t_{oi}=(t_{oi})_s=2.5$ fs, Eq. (12b). The $t_{oi}$ value is considerably lower than the Coulomb explosion time, i.e., $t_{oi}<\tau_2$. In this case the CVI conditions are satisfied and the CVI energies are obtained in the simulations for the rectangular pulse (Fig. 1). We note in passing that the proportionality $(t_{oi})_s\propto I$ for $D_{8007}$ clusters in the range $I=10^{16}$–$10^{17}\,\mathrm{W\,cm^{-2}}$ is probably not universal.

The dependence of $E_{av}$ on the pulse width $\tau$ is more complicated for the Gaussian shaped pulse (Fig. 1). At the intensity of $I=10^{17}\,\mathrm{W\,cm^{-2}}$ the dependence of the average energy $E_{av}$ versus $\tau$ for $(D)_{8007}$ exhibits a weak maximum at $\tau=10$ fs, where the ionization is complete and $E_{av}$ is very close to the CVI value (Fig. 1). The decrease of $E_{av}$, when $\tau$ decreases to $\tau=5$ fs, has the same origin as in the case of the rectangular pulse, as for this Gaussian pulse width the time of the laser field action is not sufficiently large to induce complete outer ionization. The decrease of the ion energy with increasing $\tau$, manifested at $I=10^{17}\,\mathrm{W\,cm^{-2}}$ for $\tau>10$ fs and at a larger intensity of $I=10^{18}\,\mathrm{W\,cm^{-2}}$ for $\tau>5$ fs (Fig. 1), has no analogy in the case of the rectangular pulse. In the case of the Gaussian shaped pulse, Eq. (10), the increase of the laser field $F_{\ell 0}$ at $t<0$ becomes slower with increasing the pulse width $\tau$. When the Gaussian pulse width is comparable with the time $\tau_2=13.5$ fs of the cluster radius doubling, the cluster radius may significantly increase in the domain of the field increase (at $t<0$) where outer ionization still oc-

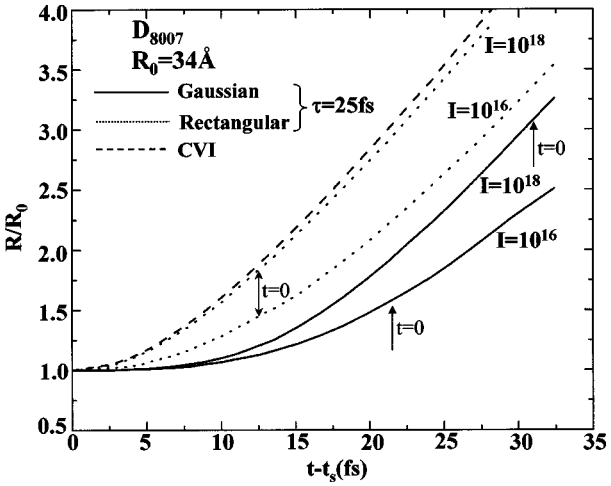


FIG. 3. Coulomb explosion dynamics, expressed by $R(t)/R_0$, of $(D)_{8007}$ clusters induced by rectangular and Gaussian pulses with $\tau$=25 fs and intensities $I=10^{16}\,\mathrm{W\,cm^{-2}}$ and $I=10^{18}\,\mathrm{W\,cm^{-2}}$. For the rectangular pulse the pulse onset occurs at $t-t_s=0$ ($t_s=-12.5$ fs), while for Gaussian pulses the peak occurs at $t=0$, which is marked on the curves. The simulation data are confronted with the CVI result, Eqs. (1) and (2). For the rectangular pulse at $I=10^{18}$ the time dependence of $R(t)/R_0$ practically coincides with the CVI results, while at the lower intensity of $I=10^{16}\,\mathrm{W\,cm^{-2}}$ marked deviations from the CVI are manifested. For the Gaussian shaped pulses, $R(t)/R_0$ manifests a considerably slower initial increase than predicted by the CVI.

curs, thus decreasing the ion energy (Paper II). For example, at $I=10^{18}\,\mathrm{W\,cm^{-2}}$ and $\tau$=100 fs, half of the electrons are removed at $t=-93$ fs (on the time scale $t\geqslant t_s<0$), when the cluster radius is ~1.7 times larger than the initial cluster radius $R_0$. Such ionization conditions are obviously far from corresponding to the CVI limit. The energy $E_{\mathrm{av}}$ for the $\tau$=100 fs laser pulse at $I=10^{18}\,\mathrm{W\,cm^{-2}}$ intensity manifests a weak isotope effect: $E_{\mathrm{av}}=1.56$, 1.67, and 1.72 keV for $(\mathrm{H})_n$, $(D)_n$, and $(\mathrm{T})_n$ $(n=8007)$ clusters, respectively. This weak isotope effect, obtained from the simulations, which marks competition between outer ionization and (mass dependent) Coulomb explosion, is in contrast with the energetics in the CVI limit for homonuclear clusters, Eq. (6), which implies the lack of isotope effects. The decrease of the ion energy with increasing $\tau$ (Fig. 1) indicates that for the Gaussian shaped pulse with a fixed peak intensity $I$, the shorter pulses in the width interval $\tau$~10–30 fs are preferable to the longer pulses of $\tau\geqslant$50 fs. The truncated laser pulse ($t_s=-\tau/2$, $F_s=0.5F_{\mathrm{M}}$) for $I=10^{17}\,\mathrm{W\,cm^{-2}}$ provides $E_{\mathrm{av}}$ energies which are only slightly lower than the CVI energies (Fig. 1).

The shape of the laser pulse significantly affects the nuclear dynamics of cluster Coulomb explosion, as demonstrated in Fig. 3 for the $D_{8007}$ cluster subjected to rectangular and Gaussian laser pulses with a width of $\tau$=25 fs. The initial time is $t_s=-0.5\tau=-12.5$ fs for the rectangular pulse, Eq. (11), and $t_s=-21.5$ and $t_s=-31$ fs at $I=10^{16}$ and at $10^{18}\,\mathrm{W\,cm^{-2}}$, respectively, for the Gaussian pulse. At a high laser intensity of $I=10^{18}\,\mathrm{W\,cm^{-2}}$ for the rectangular laser pulse, the time dependence of the cluster radius $R(t)$ almost coincides with the theoretical CVI result for the $R(t)$ dependence, inferred from Eq. (1). However, the Gaussian shaped pulse at the same laser intensity manifests a very different $R(t)$ dependence. At the beginning of the pulse, when the laser field, Eq. (10), is low, the cluster radius $R(t)$ increases much more slowly than predicted by Eq. (1). Only in the vicinity of the pulse peak ($t=21.5$ fs in Fig. 3), does the cluster radius velocity $dR/dt$ begin to increase significantly, approaching the velocity given by Eq. (1). At the lower laser intensity of $I=10^{16}\,\mathrm{W\,cm^{-2}}$ the cluster expansion is significantly retarded due to a slower and incomplete outer ionization process, which was already alluded to. The time of the cluster radius doubling for the rectangular pulse is $\tau_2=19.6$ fs, which is almost 50% larger than the theoretical value $\tau_2=13.5$ fs inferred from Eq. (3) under CVI conditions. In the case of the Gaussian pulse (Fig. 3), the cluster ionization initially starts at low laser fields and the cluster Coulomb explosion is initially slow. For this coupled laser-cluster system, the doubling time of the cluster radius $\tau_2=27$ fs (Fig. 3) is determined by the initial time $t_s$ for the simulation onset. A physically significant value of the cluster doubling time can be obtained from the time gap $\overline{\tau_2}=\tau_2-t(R/R_0=1.05)$ between the onset of cluster expansion, e.g., $t(R/R_0=1.05)$, and of $\tau_2$. For $D_{8007}$ subjected to a Gaussian pulse at $I=10^{18}\,\mathrm{W\,cm^{-2}}$, $\overline{\tau_2}=12.7$ fs, while $\overline{\tau_2}=17.7$ fs at $I=10^{16}\,\mathrm{W\,cm^{-2}}$. We note that $\overline{\tau_2}=10.9$ fs for the CVI expression, Eq. (2). As expected, the CVI expression for a Gaussian pulse provides a lower limit for $\overline{\tau_2}$.

## IV. BEYOND THE CVI APPROXIMATION

We now consider electron and nuclear dynamics in $(D)_n$ clusters, where inner ionization is complete for moderately low laser fields $I\geqslant 10^{15}\,\mathrm{W\,cm^{-2}}$ used herein (see Sec. III). In this case the deviations from the CVI conditions are solely manifested by the outer ionization process, as discussed in Paper I and in Chap. III of the present paper. Distinct features of the outer ionization electron dynamics and of the Coulomb explosion nuclear energetics will be manifested for different laser pulse shapes, which control the laser-cluster interactions.

### A. Rectangular laser pulses

Rectangular laser pulses provide a simple, although oversimplified, picture of laser-cluster interactions (Sec. III). The use of the rectangular pulse provides insight into the time scales for the applicability of the CVI. The CVI conditions are expected to be satisfied when complete outer ionization is obtained, i.e., the outer ionization time is $t_{\mathrm{oi}}=(t_{\mathrm{oi}})_s$, with the complete outer ionization time $(t_{\mathrm{oi}})$ being shorter than both the pulse width, i.e., $(t_{\mathrm{oi}})_s<\tau$, and the cluster radius doubling time $\tau_2$, i.e., $(t_{\mathrm{oi}})_s<\tau_2$ (Sec. III). With the increase of the outer ionization time (with decreasing the laser intensity or with increasing the cluster size) we expect larger deviations of the simulated average ion energy $E_{\mathrm{av}}$ from the CVI average energy $E_{\mathrm{av}}^{\mathrm{CVI}}$, Eq. (6).

Table I presents the cluster size effect on the complete outer ionization time $t_{\mathrm{oi}}$ $[\tau\geqslant t_{\mathrm{oi}}=(t_{\mathrm{oi}})_s]$ and the effect of $t_{\mathrm{oi}}$ on the simulated energy $E_{\mathrm{av}}$ for $(D)_n$ clusters ($n=459-8007$) subjected to a rectangular laser pulse with pulse width $\tau$=25 fs and intensity $I=10^{16}\,\mathrm{W\,cm^{-2}}$. From these data it is apparent that $t_{\mathrm{oi}}$ increases with increasing the cluster radius $R_0$. The condition $t_{\mathrm{oi}}<\tau_2$ (where $\tau_2=13.5$ fs)

TABLE I. Cluster size dependence of outer ionization dynamics and Coulomb explosion energetics of $(D)_n$ clusters subjected to a rectangular laser pulse ($I=10^{16}\,\mathrm{W\,cm^{-2}}$ and $\tau=25$ fs). The temporal onset of the rectangular pulse is taken at $t=0$ and the outer ionization time $t_{oi}$ is inferred from the time of the attainment of 95% of the complete outer ionization level. The $t_{oi}$ data should be compared with the cluster radius doubling time $\tau_2=13.5$ fs and $\tau_v=39.9$ fs estimated from the CVI relation, Eqs. (3) and (17). The $D^+$ ion average energies ($E_{av}$) are obtained from the simulations and the estimated energies ($E_{av}^{CVI}$) are obtained from the CVI relation, Eq. (6).

| $n$ | 459 | 959 | 1961 | 3367 | 8007 |
|---|---|---|---|---|---|
| $R_0$ (Å) | 13.1 | 16.6 | 21.1 | 25.4 | 34.0 |
| $E_{av}^{CVI}$ (keV) | 0.300 | 0.484 | 0.785 | 1.135 | 2.036 |
| $E_{av}$ (keV) | 0.294 | 0.477 | 0.748 | 1.040 | 1.729 |
| $(E_{av}^{CVI}/E_{av})-1$ | 0.02 | 0.015 | 0.05 | 0.09 | 0.18 |
| $t_{oi}$ (fs) | 3.2 | 7.3 | 10.5 | 14.4 | 25.0 |

is well satisfied for $D_{459}$ and for $D_{959}$ clusters, where for both cases the deviation between $E_{av}$ and $E_{av}^{CVI}$ is small ($\sim$2%). For larger $D_{1961}$ and $D_{3367}$ clusters, where $t_{oi}\sim\tau_2$, the deviation between the simulated value of $E_{av}$ and $E_{av}^{CVI}$ is still rather small, being 5%–9%. Only for the $D_{8007}$ cluster, with $t_{oi}\sim 2\tau_2$, the deviation becomes of some importance, being about 18% (Table I). From these data it is apparent that the CVI approximation is valid over a much wider domain of outer ionization times than those satisfying the inequality $t_{oi}<\tau_2$.

We were able to account for (first-order) deviations from the CVI equations for the energetics of Coulomb explosion of a homonuclear or uniformly expanding heteronuclear cluster induced by a rectangular pulse, where the pulse onset was defined at $t=0$. The outer ionization level (per ion) is $n_{oi}(t)=q\,\theta(t)$. We present the net positive charge (per ion) for the cluster as $n_{oi}(t)=q\,\theta(t)$, with the inner ionization being instantaneous with the charge (per ion) being $n_{ii}=q$ for all $t>0$, while the outer ionization is characterized by $\theta(t=0)=0$. For $(D)_n$ clusters $n_{ii}=q=1$ for all $t$. In the case of complete outer ionization, $\theta(t)=1$, and no unbound electrons are left inside the cluster. We define the outer ionization time $t_{oi}$ by the condition $\theta(t)<1$ for $t<t_{oi}$ and $\theta(t)=1$ for $t\geqslant t_{oi}$. The analysis of our simulation results for a rectangular pulse (see, e.g., Fig. 2) shows that the $\theta(t)$ function can be approximately represented at $t\leqslant t_{oi}$ as a power law $\theta(t)=(t/t_{oi})^{1/2}$, so we take

$$n_{oi}(t)=q(t/t_{oi})^{1/2},\quad t\leqslant t_{oi}. \tag{13}$$

An ion with a charge $q$, initially located at the distance $r_0$ from the cluster center, is subjected to a screened interaction with the other ions of an effective charge $n_{oi}(t)$. According to Eq. (13), the force acting on the reference ion is

$$F(t)=(4\pi/3)r_0^3\rho q^2(t/t_{oi})^{1/2}/r(t). \tag{14}$$

Assuming the cluster spatial expansion to be small for $t<t_{oi}$ we present the ion distance from the center at time $t$ in the form

$$r(t)=r_0(1+ct^{\kappa}),\quad ct^{\kappa}\ll 1. \tag{15}$$

Substituting Eq. (15) into Eq. (14) and solving the equation of motion, while retaining the first term in the $t$ expansion, results in $\kappa=5/2$ The ion distance from the center is then

$$r(t)=r_0\left[1+6\left(\frac{t^5}{\tau_v^4 t_{oi}}\right)^{1/2}\right],\quad t\leqslant t_{oi}, \tag{16}$$

where the CVI time parameter is

$$\tau_v=6.22q^{-1}(m/\rho)^{1/2}=2.91\tau_2. \tag{17}$$

The CVI time parameter $\tau_v$ for $(D)_n$ clusters is $\tau_v=39.9$ fs. $\tau_v$ exhibits the same pattern as $\tau_2$ for the charge dependence, the mass effect, and the lack of cluster size dependence. Using Eq. (16) we found the final average ion energy to be

$$E_{av}=E_{av}^{CVI}[1-(t_{oi}/\tau_v)^2], \tag{18}$$

where $E_{av}^{CVI}$ stands for the CVI energy, Eq. (6). From this analysis we infer that the interplay between outer ionization and Coulomb explosion yields $E_{av}<E_{av}^{CVI}$, with $(E_{av}^{CVI}-E_{av})/E_{av}=(t_{oi}/\tau_v)^2$, in semiquantitative agreement with the results of Table I. According to Eqs. (16) and (18) the CVI approximation is valid when the ionization time $t_{oi}$ is shorter than the CVI parameter $\tau_v$, i.e.,

$$t_{oi}<\tau_v. \tag{19}$$

The condition given by Eq. (19), with $\tau_v\sim 3\tau_2$, significantly extends the validity domain of the $t_{oi}$ values for the applicability of the CVI approximation for the energetics of Coulomb explosion. This conclusion concurs with the data presented in Table I for the modest deviation of the energetics from the CVI result over a wide $t_{oi}$ domain of up to $t_{oi}\sim 2\tau_2$.

Simulations of the energetics of Coulomb explosion were conducted for rectangular pulses in the intensity range $I=10^{16}$–$10^{20}\,\mathrm{W\,cm^{-2}}$. The $E_{av}$ and $E_M$ data for $I=10^{16}\,\mathrm{W\,cm^{-2}}$, while obeying the $\propto R_0^2$ scaling law show $\sim$10% deviation from the CVI (Fig. 4), due to retarded outer ionization. In the highest intensity domain $I=10^{18}$–$10^{20}\,\mathrm{W\,cm^{-2}}$, the simulation data for $E_{av}$ and $E_M$ for the rectangular pulse are intensity independent, being close to the CVI. The intensity independence of the ions energy in this range of $I=10^{18}$–$10^{20}\,\mathrm{W\,cm^{-2}}$ provides evidence for a minor effect of the direct acceleration of ions by the laser field. The same negative result is expected to apply also for other pulse shapes.

### B. Truncated Gaussian pulse

These model calculations will be useful to establish the validity domain of the CVI approximation for Coulomb explosion of $D_n$ clusters, which in this case can be practically explored by simulations for very large ($n\simeq 8\times 10^4$, $R_0=80$ Å) clusters, while such large clusters cannot be simulated for Gaussian laser pulses. The average $D^+$ ion energies, generated by a truncated Gaussian pulse, are presented in Fig. 4 over a broad size domain ($n=459$–$76\,429$). At the lower intensity of $I=10^{16}\,\mathrm{W\,cm^{-2}}$ and at the cluster size of

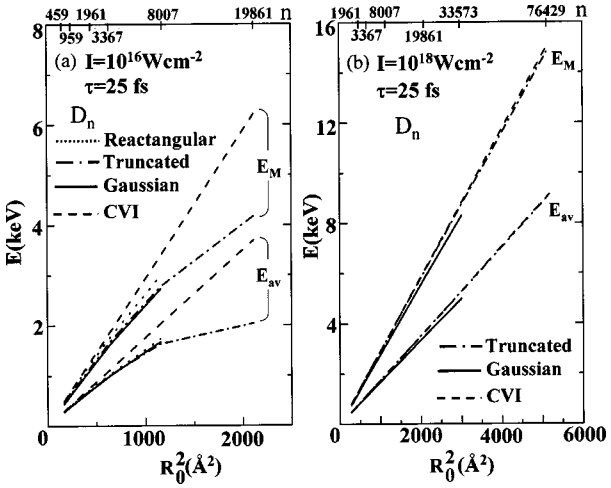


FIG. 4. Cluster size dependence of the average ($E_{av}$) and maximal ($E_M$) energies of $D^+$ ions from Coulomb explosion of $(D)_n$ clusters induced by rectangular, truncated Gaussian, and Gaussian laser pulses for laser intensities $I=10^{16}\,W\,cm^{-2}$ (a) and $I=10^{18}\,W\,cm^{-2}$ (b). The CVI results, Eqs. (6) and (7), are also presented in the figures. Note the deviations from the CVI approximation at $I=10^{16}\,W\,cm^{-2}$, which are manifested at low values of $R_0$, while at $I=10^{18}\,W\,cm^{-2}$ a good overall agreement (see text) with the CVI approximation is exhibited.

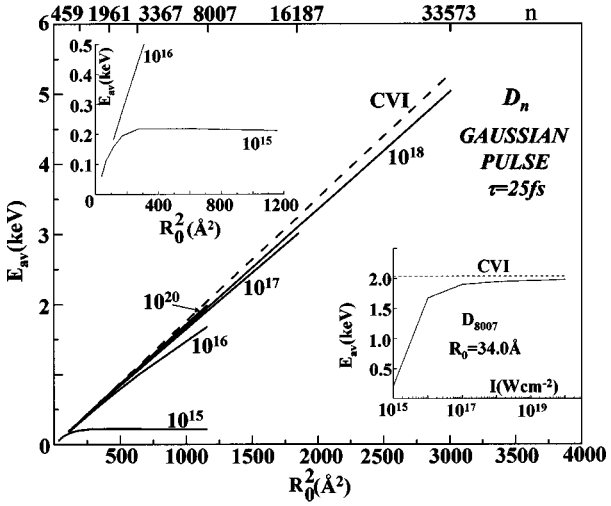


FIG. 5. Cluster size dependence of the average $D^+$ energies from Coulomb explosion of $(D)_n$ clusters ($n=459-33\,573$) induced by Gaussian pulses in the intensity range $I=10^{15}-10^{20}\,W\,cm^{-2}$ (the numbers $10^x$, $x=15-20$, on the curves mark the intensities in units of $W\,cm^{-2}$). The result of the CVI approximation, Eq. (6), is also marked. Note the overall agreement (see text) between the simulation results of the CVI approximation for the highest intensities $I=10^{18}-10^{20}\,W\,cm^{-2}$, and the intensity dependent onset of deviations from the CVI approximation for lower intensities of $I=10^{15}-10^{17}\,W\,cm^{-2}$ (see text). The left-hand side inset shows the size dependent energetics at these lower intensities of $I=10^{15}-10^{16}\,W\,cm^{-2}$, where a break from the CVI approximation for $I=10^{15}\,W\,cm^{-2}$ is already exhibited for $R_0\simeq 8-10$ Å. The right-hand side inset shows the intensity dependence of the Coulomb explosion energy of $(D)_{8007}$, which nearly converges to the CVI result for $I\gtrsim 3\times 10^{17}\,W\,cm^{-2}$.

$n\leqslant 8000$, the simulated average energy $E_{av}$, and the maximal energy $E_M$ for the truncated, the rectangular, and the Gaussian pulses, [Fig. 4(a)] exhibit a linear $E_{av}\propto R_0^2$ and $E_M\propto R_0^2$ dependence, in qualitative agreement with the CVI size equations, Eqs. (6) and (7). However, the slopes of these $E_M$, $E_{av}\propto R_0^2$ curves at $I=10^{16}\,W\,cm^{-2}$ are lower by 16%–24% than the slope expected for the CVI [Fig. 4(a)]. At $n>8000$ a break of the linear $E_M$ and $E_{av}$ versus $R_0^2$ relation is exhibited. For $n>8000$, $E_M$ and $E_{av}$ (induced by the truncated pulse) continue to increase with increasing $R_0^2$, although the increase is slower than for $n<8000$ [Fig. 4(a)]. This trend reflects on the quantitative breakdown of the CVI for the ion energetics at the lower $I=10^{16}\,W\,cm^{-2}$ intensity. At the higher intensity of $I=10^{18}\,W\,cm^{-2}$, the $E_M$, $E_{av}\propto R_0^2$ relation is well obeyed over a broad cluster size domain of [$n=1961-76\,429$, Fig. 4(b)]. The simulated average energy $E_{av}$ nearly coincides with the CVI equation, Eq. (6), for the entire range of cluster radii studied herein (over the size domain of $n=459-8\times 10^4$), quantitatively confirming the validity of the cluster size dependence of the CVI [Fig. 4(b)]. The simulated maximal energy $E_M$ is again close to the CVI maximal energy, Eq. (7).

### C. Gaussian shaped pulses

The exploration of the energetics of Coulomb explosion induced by Gaussian laser pulses is of considerable interest. From the practical point of view, these results are relevant for the sake of a comparison with experiment. Simulations using Gaussian pulses (Fig. 5) allow us to establish the convergence of the simulation results to the CVI results for the energetics of Coulomb explosion of $(D)_n$ clusters in the intensity range of $I=10^{15}-10^{20}\,W\,cm^{-2}$ (with pulse width $\tau=25$ fs). The intensity range of $I=10^{15}-10^{16}\,W\,cm^{-2}$ marks the onset of effective outer ionization and of Coulomb explosion, which exhibits a marked cluster size and pulse intensity dependence of the energetics (Fig. 5). At the lowest intensity of $I=10^{15}\,W\,cm^{-2}$ the energy initially increases and then saturates at very small cluster sizes of $R_0\gtrsim 10$ Å, corresponding to $n\gtrsim 200$ (left-side inset to Fig. 5). At the intensity of $I=10^{16}\,W\,cm^{-2}$, a more effective outer ionization for somewhat larger clusters allows for the increase of the energy with increasing $R_0$. At $I=10^{16}\,W\,cm^{-2}$ $E_{av}$ increases with increasing the size, i.e., $E_{av}\propto R_0^2$ for $n\sim 400-3000$, and then $E_{av}$ tends toward saturation for $n>8000$ (Fig. 5). For moderately sized $D_{8007}$ clusters, $E_{av}$ increases fast with increasing $\log I$ in the range $I=10^{15}-10^{17}\,W\,cm^{-2}$ due to enhancement of (complete or incomplete) outer ionization with increasing $I$ (right-side inset to Fig. 5). Subsequently, for $I\gtrsim 10^{17}\,W\,cm^{-2}$ a saturation of $E_{av}$ versus $I$ is exhibited, nearly converging to the CVI result (right-side inset to Fig. 5).

The marked features of the energetics of Coulomb explosion in the intensity range of $I=10^{15}-10^{20}\,W\,cm^{-2}$ over the cluster size domain studied herein (Fig. 5) are (a) the existence of a finite, laser intensity dependent, range of $E_{av}\propto R_0^2$ cluster size dependence; (b) the applicability of the CVI for the $E_{av}\propto R_0^2$ size dependence is realized for $R_0<(R_0)_I$, and the breakdown of the CVI occurs for $R_0>(R_0)_I$. The applicability range of the CVI is characterized by the boundary radius $(R_0)_I$ at intensity $I$; and (c) the near-convergence of $E_{av}$ to the CVI result, Eq. (6), for a fixed sized cluster is realized with increasing the peak intensity of the Gaussian pulse.

Coulomb explosion of $D_n$ clusters subjected to a Gaussian pulse of a high $I \geqslant 10^{18}\,\mathrm{W\,cm^{-2}}$ intensity provides $D^+$ average energies, which are somewhat lower than the CVI energy (Figs. 1 and 5). The relative differences between these simulated and CVI energies correspond to ~5% for the pulse width of $\tau=25$ fs (Fig. 5) and ~20% for $\tau=100$ fs (Fig. 1). Although the Gaussian pulses at $I \geqslant 10^{18}\,\mathrm{W\,cm^{-2}}$ do not provide CVI energies, in the high intensity domain they do demonstrate two features typical for such CVI energetics, Eq. (6): First, the scaling law $E_{\mathrm{av}} \propto R_0^2$ is exhibited over a broad cluster size domain. However, the slope of the linear $E_{\mathrm{av}} \propto R_0^2$ curve exhibits some deviations from the CVI. Second, the $E_{\mathrm{av}} \propto R_0^2$ relation does not depend (or only weakly depends) on the laser intensity (Fig. 5). Thus for Gaussian pulses in the high intensity domain, the CVI is not rigorously applicable, but constitutes a reasonable working hypothesis over a well defined, broad cluster size domain. We shall refer to this high intensity region ($I \geqslant 10^{18}\,\mathrm{W\,cm^{-2}}$) for $D_n$ clusters subjected to Gaussian pulses considered herein as a pseudo-CVI domain, which will subsequently be discussed.

## V. OUTER IONIZATION DYNAMICS AND THE BOUNDARY RADIUS FOR THE CVI DOMAIN

We shall now relate to the electron dynamics for outer ionization and nuclear dynamics for Coulomb explosion of $D_n$ clusters subjected to Gaussian pulses. The outer ionization dynamics in the pseudo-CVI domain can be described in terms of a simple electrostatic model[16,36] for cluster barrier suppression [Eq. (13) of Paper I]. This model implies that the total (positive) cluster charge is $Q_I(t)=qN_{\mathrm{oi}}(t)$, with $N_{\mathrm{oi}}(t)=nn_{\mathrm{oi}}(t)$, being the total number of outer ionized electrons, where $n[=(4\pi/3)\rho R_0^3]$ is the number of constituents and $n_{\mathrm{oi}}(t)$ is the outer ionization level (per constituent). $Q_I(t)$ is determined by the relation $eF_{\ell 0}(t)=\sqrt{2}BQ_I^{(t)}/[R(t)]^2$, where $R(t)$ is the cluster radius at time $t$ and $F_{\ell 0}(t)$ is the laser field envelope amplitude at this time (Paper I). Accordingly, during outer ionization, when $N_{\mathrm{oi}}(t) \leqslant n$, $n_{io}(t)$ is given by

$$n_{\mathrm{oi}}(t)=eF_{\ell 0}(t)[R(t)]^2/\sqrt{2}Bqn. \tag{20}$$

The time evolution of the fraction of outer ionization (per D atom) and of the cluster radius is obtained from molecular dynamics simulations for the electron-nuclear-laser system (Paper II), which provides the time dependence of $n_{\mathrm{oi}}(t)$ and of $R(t)$. Using Eq. (20) (with $q=1$ and $\rho=0.05$ $\mathrm{\AA^{-3}}$), together with the numerical simulations of $R(t)$, we obtained the results for $n_{\mathrm{oi}}(t)$. In Fig. 6 we confront the results for $n_{\mathrm{oi}}(t)$, as obtained from Eq. (20) and from the simulations of electron dynamics in $D_{8007}$ clusters, using different laser Gaussian pulse parameters. When the laser pulse parameters fall in the range appropriate for the pseudo-CVI behavior, i.e., $I=10^{18}$–$10^{20}\,\mathrm{W\,cm^{-2}}$ and $\tau=25$–50 fs, the outer ionization is complete [$n_{\mathrm{oi}}(t) \to 1$ with increasing $t$]. Under these circumstances good agreement between the electrostatic model, Eq. (20), and the simulation results is obtained over the range $0.15 < n_{\mathrm{oi}}(t) < 0.95$ (Fig. 6). The description of the outer ionization process by Eq. (20) implies that the ionization of the nanoplasma adiabatically follows the laser field $F_{\ell 0}(t)$ and the increase of the cluster radius.

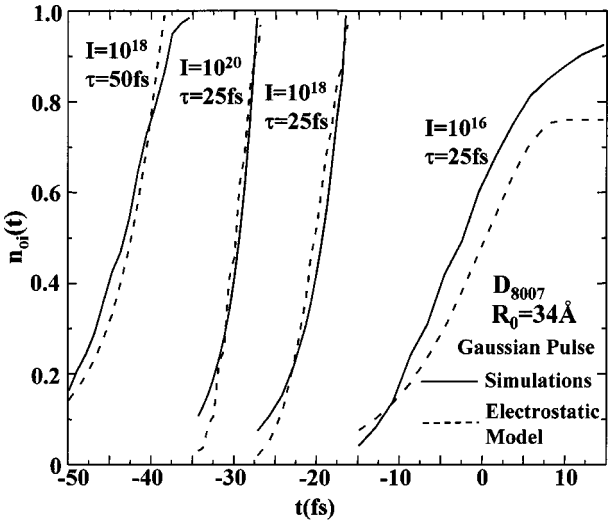


FIG. 6. Electron dynamics for the outer ionization level of $(D)_{8007}$ clusters induced by Gaussian pulses with $\tau=25$ and 50 fs and $I=10^{16}$–$10^{18}\,\mathrm{W\,cm^{-2}}$ (the numbers $10^x$, $x=16$–20, represent intensities in $\mathrm{W\,cm^{-2}}$). The simulation results for the outer ionization level (per atom) are confronted with the prediction of the electrostatic model, Eq. (20).

Such an outer ionization process involves ionization induced by adiabatic following of the laser field and of the cluster size (IIAFLS). For a Gaussian pulse, the IIAFLS mechanism is realized at a high laser intensity ($I \geqslant 10^{18}\,\mathrm{W\,cm^{-2}}$) provides a pseudo-CVI behavior, with the resulting nuclear energetics being close to the strict CVI behavior. The nuclear dynamics and energetics induced by a Gaussian pulse will be referred to as a pseudo-CVI (rather than CVI) behavior, as the electron dynamics and the outer ionization adiabatically follow the laser field. At a lower intensity of $I=10^{16}\,\mathrm{W\,cm^{-2}}$ the outer ionization dynamics in the $D_{8007}$ cluster induced by a Gaussian pulse significantly differs from the IIAFLS mechanism (Fig. 6), violating the pseudo-CVI energetics (Fig. 5). According to the simulation results for $I=10^{16}\,\mathrm{W\,cm^{-2}}$ (Fig. 5) the deviation from the $E_{\mathrm{av}} \propto R_0^2$ relation sets in for small clusters, and becomes noticeable (e.g., about 7%) for $R_0=21\,\mathrm{\AA}$ ($n=1961$), when the outer ionization is almost complete.

The condition for nearly complete outer ionization can be obtained from the electrostatic model, Eq. (20), and will provide alternative estimates for the boundary radius $(R_0)_I$ (Sec. IV). When outer ionization is complete, we expect that (at the laser intensity $I$) the CVI relation is applicable for $R_0 < (R_0)_I$ and breaks down for $R_0 > (R_0)_I$. Thus $(R_0)_I$, defined on the basis of electron dynamics, marks the boundary radius for the applicability of the pseudo-CVI behavior. To provide a quantitative characterization for this boundary radius, we shall define the cluster size $(R_0)_I$ as the initial radius $R_0$ of a cluster where, at the peak of the Gaussian laser field, Eq. (10), $F_{\ell 0}(t=0)=F_{\mathrm{M}}$, the outer ionization level is 95%, i.e., $n_{\mathrm{oi}}(t=0)=0.95$. Equation (20), together with $q=1$, $n=(4\pi/3)\rho R_0^3$, $eF_{\ell 0}(t=0)=eF_{\mathrm{M}}$, and the relation $eF_{\mathrm{M}}=2.75\times 10^{-7}I^{1/2}$, results in the following relation:

$$(R_0)_I=eF_{\mathrm{M}}/\sqrt{2}(4\pi/3)B\rho q\xi_0^2 = 3.3\times 10^{-9}I^{1/2}/\rho q\xi_0^2, \tag{21}$$

where

$$\xi_0 = R_0/R(t=0). \tag{22}$$

Here $R(t=0)$ is the cluster radius at the peak of the Gaussian laser intensity. The simulation results demonstrate a weak laser intensity dependence of the parameter $\xi_0$ for clusters of the size $(R_0)_I$, at least for $I \geqslant 10^{16}\,\mathrm{W\,cm^{-2}}$. This parameter is $\xi_0 = 0.55$ at $I = 10^{16}\,\mathrm{W\,cm^{-2}}$ and $\xi_0 \approx 0.54$ [found by extrapolation of the $\xi_0(R_0)$ dependence] at $I = 10^{17}\,\mathrm{W\,cm^{-2}}$. Very rough extrapolation provides $\xi_0 \sim 0.45$–$0.6$ at $I = 10^{18}\,\mathrm{W\,cm^{-2}}$. Provided that the cluster size expansion parameter $\xi_0$ exhibits a weak intensity dependence, we expect that $(R_0)_I \propto I^{1/2}$.

Two independent estimates of the boundary radius $(R_0)_I$ can be obtained from our simulation results:

(1) Simulations for the energetics provide the ranges of $R_0$ where the $E_{\mathrm{av}} \propto R_0^2$ relation breaks down. These ranges of $R_0$ give rough estimates of $(R_0)_I$ [see point (b) in Sec. IV above]. Our simulations for the energetics for $(D)_n$ clusters induced by a Gaussian pulse (Sec. IV and Fig. 5) accordingly give $(R_0)_I \sim 5$–$8$ Å for $I = 10^{15}\,\mathrm{W\,cm^{-2}}$, $(R_0)_I \sim 20$–$30$ Å for $I = 10^{16}\,\mathrm{W\,cm^{-2}}$, $(R_0)_I > 43$ Å for $I = 10^{17}\,\mathrm{W\,cm^{-2}}$ and $(R_0)_I \gg 60$ Å for $I = 10^{18}\,\mathrm{W\,cm^{-2}}$.

(2) Simulations of the outer ionization level. $(R_0)_I$ is obtained from the simulation results for the attainment of complete outer ionization, i.e., $n_{\mathrm{oi}}(t=0) = 0.95$. The $(R_0)_I$ radii defined this way can be provided directly from our simulation results for the electron dynamics at the two lower intensities only, i.e., $I = 10^{15}\,\mathrm{W\,cm^{-2}}$ with $(R_0)_I = 5.8$ Å, and $I = 10^{16}\,\mathrm{W\,cm^{-2}}$ with $(R_0)_I = 20.4$ Å. For the larger intensity of $I = 10^{17}\,\mathrm{W\,cm^{-2}}$ we found the laser fields $F_{\ell 0}$, which provide an almost complete (95%) ionization level ($n_{\mathrm{oi}} = 0.95$) for different cluster radii $R_0$, and extrapolated this dependence to $F_{\ell 0} = F_{\mathrm{M}}$. Using such an extrapolation procedure we found $(R_0)_I = 76.5$ Å for $I = 10^{17}\,\mathrm{W\,cm^{-2}}$. At $I = 10^{18}\,\mathrm{W\,cm^{-2}}$ the $(R_0)_I$ radius is so large that no extrapolation of our simulation results can be conducted.

To provide a rough estimate for the boundary radii $(R_0)_I$ we utilize the simulation result $(R_0)_I = 20.4$ Å for $I = 10^{16}\,\mathrm{W\,cm^{-2}}$ (from the simulation of the outer ionization level). This value of $(R_0)_I$ is then consistent with the corresponding result inferred from Eq. (21), provided that $\xi_0 = 0.55$. We now invoke the assumption that the parameter $\xi_0$ is independent of the laser intensity. Using Eq. (21) with $q = 1$, $\rho = 0.05$ Å$^{-3}$ (per $D$ atom) and $\xi_0 = 0.55$ results in the following numerical relations:

$$(R_0)_I = 2.2 \times 10^{-7} I^{1/2}, \tag{23}$$

where $(R_0)_I$ is presented in Å and $I$ in $\mathrm{W\,cm^{-2}}$. The values of $(R_0)_I$ evaluated from Eq. (23) are presented in Fig. 7, where we also display the values of the cluster sizes $(n)_I = (4\pi/3)\rho(R_0)_I^3$ that correspond to the boundary radii. In Fig. 7 we compare the analytical results of $(R_0)_I$ for $(D)_n$ clusters based on the predictions of the electrostatic model, Eqs. (21) and (23), with the estimates of $(R_0)_I$ inferred from simulations of the energetics as well as from simulations of the outer ionization level. The overall agreement between the electrostatic model and the simulation results for both energetics and electron dynamics inspires confidence in our physical picture.

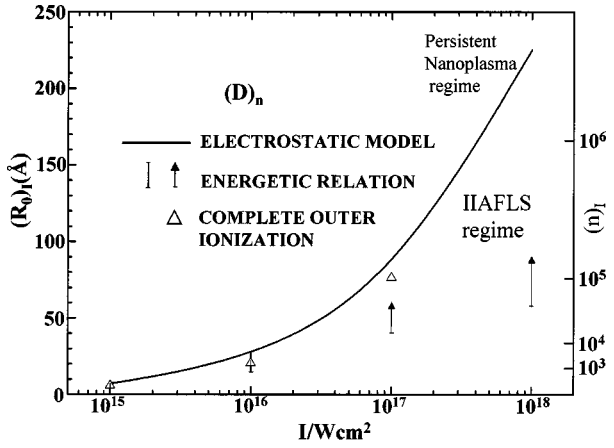


FIG. 7. The boundary cluster radii $(R_0)_1$ for the applicability of the pseudo-CVI for Gaussian pulses in the intensity range of $I = 10^{15}$–$10^{18}\,\mathrm{W\,cm^{-2}}$. We present the simulation results for nuclear dynamics, marking the breakdown of the CVI energy relation $E_{\mathrm{av}} \propto R_0^2$ (presented by the range I and by the lower limit ↑), and the simulation results for electron dynamics, marking a complete (95%) level of outer ionization (open triangles). The solid line presents the prediction of the electrostatic model, Eq. (23), which separates between the IIAFLS regime and the persistent plasma regime.

Another interesting result for the characterization of the IIAFLS regime involves the relation between the boundary cluster radius $(R_0)_I$ and the corresponding average ion energy $(E_{\mathrm{av}})_I$ for Coulomb explosion of this cluster at the same laser intensity. In the pseudo-CVI regime our simulations (Fig. 5) at $R_0 < (R_0)_I$ result in the relation $E_{\mathrm{av}} \propto R_0^2$, whereupon at the boundary radius we expect the quadratic relation $(E_{\mathrm{av}})_I \propto (R_0)_I^2$ to hold. Using Eq. (21) for $(R_0)_I$ and the CVI result, Eq. (6), as a reasonable approximation for $(E_{\mathrm{av}})_I$, leads to the relation

$$(E_{\mathrm{av}})_I = (9/40\pi)\frac{(eF_{\mathrm{M}})^2}{B\rho\xi_0^4}. \tag{24}$$

Taking again $\xi_0 = 0.55$ and $\rho = 0.05$ Å$^{-3}$ results in the approximate numerical relation

$$(E_{\mathrm{av}})_I = 8.2 \times 10^{-14} I, \tag{25}$$

where $(E_{\mathrm{av}})_I$ is presented in eV and $I$ in $\mathrm{W\,cm^{-2}}$. The proportionality relation $(E_{\mathrm{av}})_I \propto I$ is well obeyed for the simulation data for the average energies of $(D)_n$ clusters, which correspond to 95% of the outer ionization levels. These simulation results give $(E_{\mathrm{av}})_I$ values of 0.053, 0.67, and 6.8 keV for $I = 10^{15}$, $10^{16}$, and $10^{17}\,\mathrm{W\,cm^{-2}}$, respectively. These simulation values of $(E_{\mathrm{av}})_I$ are lower by about 17%–35% than those estimated from Eq. (25). To establish the interrelationship between $(E_{\mathrm{av}})_I$ and $(R_0)_I$, (Fig. 8), we have used an extrapolation procedure by taking a single pair of $(R_0)_{\tilde{I}} = 20.4$ Å and $(E_{\mathrm{av}})_{\tilde{I}} = 0.67$ keV values at $\tilde{I} = 10^{16}\,\mathrm{W\,cm^{-2}}$ obtained from our simulations, together with other $(R_0)_I$ values inferred from the electrostatic model (Fig. 7) in the intensity range $I = 10^{15}$–$10^{20}\,\mathrm{W\,cm^{-2}}$, to estimate the corresponding $(E_{\mathrm{av}})_I$ values from the quadratic relation $(E_{\mathrm{av}})_I = (E_{\mathrm{av}})_{\tilde{I}}(R_0)_I^2/(R_0)_{\tilde{I}}^2$. In Fig. 8 we present the results for the

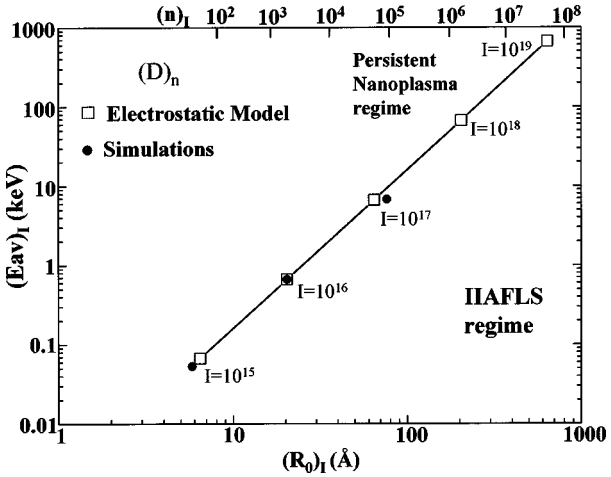


FIG. 8. The relation of the boundary cluster radius $(R_0)_I$ for the applicability of the pseudo-CVI and the corresponding average ion energy $(E_{av})_I$ for Gaussian pulses in the intensity range $I=10^{15}-10^{19}\,\mathrm{W\,cm^{-2}}$. The simulation results, marking a complete (95%) level of outer ionization, are represented by black dots. The predictions of the electrostatic model, scaled according to the $(E_{av})_I \propto (R_0)_I^2$ relation (see text), are represented by open squares. The solid line, which connects the data of the electrostatic model, separates between the IIAFLS regime and the persistent nanoplasma regime.

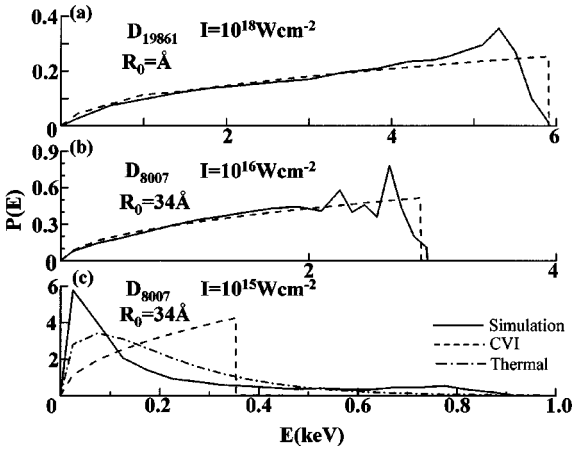


FIG. 9. Energy distribution of $D^+$ ions from Coulomb explosion of $(D)_n$ ($n=8007$ and 19 861) clusters induced by a Gaussian laser pulse ($I=10^{15}-10^{18}\,\mathrm{W\,cm^{-2}}$). The simulation results at $I=10^{18}\,\mathrm{W\,cm^{-2}}$ and $I=10^{16}\,\mathrm{W\,cm^{-2}}$ are in accord with the prediction of the CVI, Eq. (8). At the low intensity of $I=10^{15}\,\mathrm{W\,cm^{-2}}$, marked deviations from the CVI are exhibited.

quadratic relation between $(E_{av})_I$ and $(R_0)_I$ incorporating $(R_0)_I$ data from the electrostatic model and from our simulations, together with the $(E_{av})_I$ data from extrapolation and from simulations. The data of Fig. 8 are useful to assess the validity range of the pseudo-CVI size domain for the production of energetic $D^+$ ions from Coulomb explosion of $(D)_n$ clusters at different laser intensities.

Another prediction of the electrostatic model pertains to the saturation of $E_{av}$ toward $E_{av}^{CVI}$ with increasing $I$ at a fixed cluster radius $R_0$. Such data are presented in Fig. 5 (right-side inset) for $R_0=34$ Å. This saturation is expected to be exhibited at the intensity which corresponds to $R_0<(R_0)_I$. From the intensity dependence of the boundary radius $(R_0)_I$ (Figs. 7 and 8) we infer that the simulation data for a fixed $R_0=34$ Å value should exhibit a saturation of $E_{av}/E_{av}^{CVI}\rightarrow 1$ for $I\geqslant 3\times 10^{16}\,\mathrm{W\,cm^{-2}}$. Indeed, this conclusion concurs with the simulation results (right-side inset to Fig. 5).

From the present analysis we conclude that the violation of the IIAFLS conditions, which is caused by incomplete outer ionization and by the screening of the interionic repulsion by nanoplasma electrons (see Paper II), is manifested by the breakdown of the $E_{av}\propto R_0^2$ pseudo-CVI relation at fixed $I$ with increasing $R_0$ and by the deviation of the simulated value of $E_{av}$ from the CVI result. It is satisfactory that the electrostatic model accounts for the validity range of the pseudo-CVI for the size dependence of the energetics at fixed $I$ and for the intensity dependence for the attainment of the CVI energy at a fixed cluster size.

The character of the outer ionization process significantly affects the energy distribution of the product ions induced by a Gaussian pulse ($\tau=25$ fs) (Fig. 9). In the IIAFLS domain at $I=10^{18}\,\mathrm{W\,cm^{-2}}$ (where $R_0<(R_0)_I=220$ Å) and even when the IIAFLS conditions are noticeably, but not very strongly, violated as in the $D_{8000}$ cluster ($R_0=35$ Å $>(R_0)_I$ at $I=10^{16}\,\mathrm{W\,cm^{-2}}$), the ion energy distribution is similar to the CVI distribution of Eq. (8), i.e., $P(E)\propto E^{1/2}$ (Fig. 9). Only when the IIAFLS conditions are strongly violated, as in the case of the $D_{8007}$ cluster at $I=10^{15}\,\mathrm{W\,cm^{-2}}$ [$R_0\gg(R_0)_I=7$ Å], the energy distribution strongly deviated from the CVI distribution and roughly followed the thermal distribution of the form $P(E)\propto E^{-1/2}\exp(-E/E_{av})$ (Fig. 9).

## VI. CONFRONTATION WITH EXPERIMENTAL DATA

The currently available experimental data for deuterium cluster sizes used in multielectron ionization and Coulomb explosion are not very reliable.[48,49] In view of the $E_{av}\propto R_0^2$ cluster size dependence of the average $D^+$ ion energy in the CVI and in the pseudo-CVI domains (Chaps. IV and V), even a moderate uncertainty in the cluster radius may lead to a significant variation in the Coulomb explosion energies. Furthermore, the lack of reliable parameters, which describe the distribution of the cluster radii, hampers the comparison of our simulation results with the experimental data.

Our simulation results for the $D^+$ average energies from Coulomb explosion of $(D)_n$ clusters (Fig. 5) will be confronted with the experimental data of Madison *et al.*[30] The experimental $D^+$ average energies at the laser energy of 0.1J (peak intensity of $I\sim 2\times 10^{18}\,\mathrm{W\,cm^{-2}}$) lie in the interval $E_{av}=5-7$ keV.[30] According to our simulations at $I=10^{18}\,\mathrm{W\,cm^{-2}}$ (Fig. 5), this energy interval corresponds to the cluster radii range $R_0=54-64$ Å (where the $R_0$ value was obtained from the $E_{av}\propto R_0^2$ extrapolation). Using the log-normal size distribution of Madison *et al.*,[30] we estimated that the average cluster radii $\bar{R}_0$, which provide the $E_{av}=5-7$ keV energies, correspond to $R_0=51-60$ Å. The average cluster radius found in Ref. 30 by fitting the time-of-flight signals of the ions was $\bar{R}_0=45$ Å. This value is lower (by 10%–25%) than our estimate, which rests on the energetic simulation data.

Our simulation results may underestimate the $D^+$ ion energies. However, the simulated $E_{av}$ data are only slightly lower (by less than 5%) than the CVI energies (Fig. 5),

TABLE II. Anisotropy of $D^+$ ion velocities for Coulomb explosion of $(D)_n$ clusters. The anisotropy parameter $\theta=2\langle v_x\rangle/(\langle v_y\rangle+\langle v_z\rangle)$ is expressed in terms of the mean square averaged velocity components $\langle v_j\rangle$ along the $j=x$, $y$, and $z$ axes. The laser pulse propagates along the $z$ axis and the polarization direction is along the $x$ axis. Simulations of electron and nuclear dynamics were performed for the Gaussian pulse ($\tau=25$ fs), while simulations of nuclear dynamics were performed for vertically ionized clusters subjected to a rectangular laser field ($\tau=25$ fs). The velocity components are identical along the $y$ and $z$ axes.

| | $\theta$ for Gaussian pulse | | | | | $\theta$ for CVI |
|---|---|---|---|---|---|---|
| $n\backslash I(\mathrm{W\,cm^{-2}})$ | $10^{15}$ | $10^{16}$ | $10^{17}$ | $10^{18}$ | $10^{20}$ | $10^{20}$ [a,b] |
| 959 | 1.092 | 1.069 | 1.062 | 1.057 | 1.047 | 1.000 |
| 3367 | 1.103 | 1.086 | 1.070 | 1.063 | 1.053 | 1.000 |

[a]Simulations for vertically ionized clusters subjected to a rectangular laser field of $I=10^{20}\,\mathrm{W\,cm^{-2}}$.

[b]Test simulations were also performed for vertically ionized clusters at zero field, which resulted in $\theta=1.000$.

which provide the maximal ion energy $E_{\mathrm{av}}$ for a given value of $R_0$ (or a minimal value of $R_0$ for a given value of $E_{\mathrm{av}}$). Using the CVI energies [Eq. (6) and Fig. 5] and, after correcting the log-normal size distribution, we obtained the mean cluster radii ranges of $\bar{R}_0=49-58$ Å, which are still higher than the $R_0$ value reported in Ref. 30. The discrepancy between the simulated and the experimental $\bar{R}_0$ values most probably indicates that the experimental average cluster radius $R_0$ of Madison *et al.*[30] may have been underestimated.

Our simulation results exhibit anisotropy in the angular distribution of the $D^+$ ions. The anisotropy parameter $\theta=2\langle v_x\rangle/(\langle v_y\rangle+\langle v_z\rangle)$ for the velocities of $D^+$ ions from the Coulomb explosion of $(D)_n$ $(n=959, 3367)$ clusters (Table II), is expressed in terms of the mean squared velocity components $\langle v_j\rangle(j=x,y,z)$ with the laser pulse propagation along the $z$ axis and the polarization direction along the $x$ axis. The anisotropy parameters for a Gaussian pulse in the intensity range $I=10^{15}-10^{20}\,\mathrm{W\,cm^{-2}}$ reveal a velocity increase of 5%–10% along the polarization axes of the laser field with $\theta=1.05-1.10$, relative to the ions moving along the other two perpendicular axes (Table II). Consequently, the kinetic energy will reveal an anisotropy of 10%–20% along the laser polarization axes. From the results of Table II the cluster size effects in the narrow size domain explored therein are small at a fixed intensity. They are somewhat lower ($\theta=1.04-1.06$) for the highest intensities of $I=10^{18}-10^{20}\,\mathrm{W\,cm^{-2}}$, where the pseudo-CVI behavior prevails, than for the lower intensities of $I=10^{15}-10^{16}\,\mathrm{W\,cm^{-2}}$ ($\theta=1.07-1.10$), where the persistent nanoplasma prevails. The anisotropy parameter increases with decreasing the laser intensity, demonstrating the effect of the enhancement of the outer ionization of the nanoplasma in reducing the anisotropy of the angular distribution. For the CVI limit in the presence of a laser field at $I=10^{20}\,\mathrm{W\,cm^{-2}}$, no anisotropy effects are manifested (Table II). Accordingly, the complete simulation of the anisotropy in the angular distribution, velocities and kinetic energies of $D^+$ ions in the highest intensity range of $I=10^{18}-10^{20}\,\mathrm{W\,cm^{-2}}$, manifest deviations from the CVI, marking the role of the response of the nanoplasma in the pseudo-CVI domain. The lack of anisotropy in the CVI limit demonstrates that the effect of driving the ions by the laser field is negligible (see also Sec. IV A). The prediction of the 12% anisotropy of the kinetic energy of $D^+$ ions energy at $I=10^{18}\,\mathrm{W\,cm^{-2}}$ (Table II) fits well with the ~15% in the experimental ion energies detected by Madison *et al.*[30] in the explosion of $(D)_n$ clusters at $I=\sim10^{18}\,\mathrm{W\,cm^{-2}}$ (see Fig. 4 of Ref. 30). A further experimental search for this angular anisotropy will be of interest.

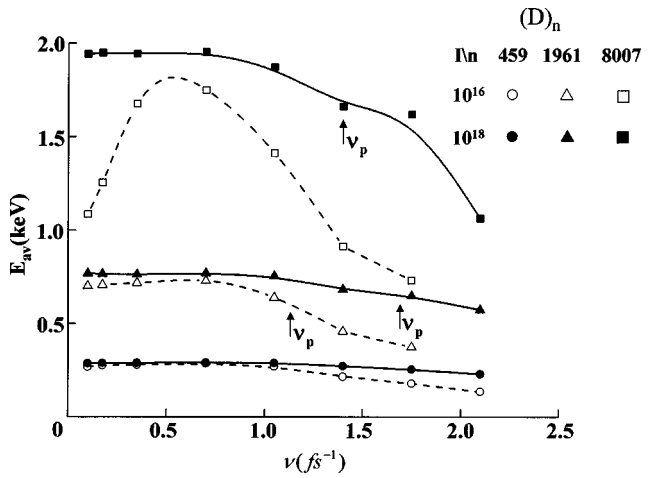


FIG. 10. Laser frequency dependence of the energetics of $D^+$ ions from Coulomb explosion of $(D)_n$ $(n=459-8007)$ clusters induced by Gaussian pulses in the intensity range $I=10^{16}-10^{18}\,\mathrm{W\,cm^{-2}}$. The characteristic frequencies $\nu_p$, which represent the upper limits for a nearly flat frequency dependence of $E_{\mathrm{av}}$, are marked by arrows.

## VII. LASER FREQUENCY DEPENDENCE OF THE ENERGETICS OF COULOMB EXPLOSION

In Chaps. III–VI of the present paper, as well as in the previous Papers I and II, the simulations of electron and nuclear dynamics have been performed for a fixed laser frequency of $\nu=0.35$ fs$^{-1}$ (laser wavelength of $\lambda=860$ nm), which corresponds to a typical IR frequency of ultraintense lasers. The dependence of the cluster electron and nuclear dynamics on the laser frequency is of inherent and practical interest. To address this issue, we performed simulations of Coulomb explosion of $(D)_n$ $(n=459-8007)$ clusters, which was induced by ultraintense laser fields ($I=10^{16}-10^{18}\,\mathrm{W\,cm^{-2}}$) over a broad laser frequency range of $\nu=0.1-2.1$ fs$^{-1}$ ($\lambda=3000-140$ nm).

The dependence of the average energies $E_{\mathrm{av}}$ of $D^+$ ions on the laser frequency is portrayed in Fig. 10 for $D_n$ clusters with $n=459$, 1961, and 8007 ($R_0=13.1$, 21.1, and 34.0 Å, respectively), subjected to laser intensities of $I=10^{16}\,\mathrm{W\,cm^{-2}}$ and $I=10^{18}\,\mathrm{W\,cm^{-2}}$. In all cases presented in Fig. 10, with the exception of the largest $(D)_{8007}$ cluster at the lower $I=10^{16}\,\mathrm{W\,cm^{-2}}$ intensity, the $E_{\mathrm{av}}(\nu)$ versus $\nu$ dependence is nearly flat with increasing $\nu$, up to a characteristic frequency of $\nu_p$, with $E_{\mathrm{av}}(\nu)$ decreasing with increasing $\nu$ for $\nu>\nu_p$. This characteristic frequency $\nu_p$ was (arbitrarily) defined as the frequency for which $E_{\mathrm{av}}(\nu)$ is lower by about 15% than the maximal value of $E_{\mathrm{av}}(\nu<\nu_p)$. The $\nu_p$ values, which are marked in Fig. 10, depend very weakly on the laser intensity (increasing as $I^{0.07}$, with increasing $I$), and decrease with increasing the cluster radius

(roughly as $R_0^{-0.2}-R_0^{-0.4}$). The flat $E_{\mathrm{av}}(\nu)$ versus $\nu$ dependence at $\nu<\nu_p$ is in accord with the electrostatic model (Chap. IV of Paper I and Sec. V of the present paper). This model describes the cluster outer ionization process in the pseudo-CVI regime, with the transient nanoplasma within the cluster being of a sufficient short lifetime on the time scale of Coulomb explosion. According to our simulations for all the clusters studied herein, which exhibit the flat $E_{\mathrm{av}}(\nu)$ versus $\nu$ dependence, the transient nanoplasma is indeed observed and the dependence of $E_{\mathrm{av}}$ on the laser intensity $I$ and the cluster radius $R_0$ is typical for the pseudo-CVI regime (as in Fig. 5 for $\nu=0.35\ \mathrm{fs}^{-1}$). The domain $\nu<\nu_p$ seems to correspond to the laser period $\tau_\ell=1/\nu$, being considerably longer than the time $\tau_{C\ell}$ of an electron moving through the cluster, whereupon when $\tau_{C\ell}<\tau_\ell$, $E_{\mathrm{av}}(\nu)$ is nearly independent of $\nu$.

The situation is quite different for the $D_{8007}$ cluster at $I=10^{16}\,\mathrm{W\,cm^{-2}}$ (Fig. 10), whose characteristics markedly deviate from the pseudo-CVI behavior (Fig. 5). In this case, the $E_{\mathrm{av}}(\nu)$ versus $\nu$ dependence demonstrates a wide maximum, which most probably indicates some quasiresonance ionization process (Chap. IV of Paper II and Ref. 16). Under these circumstances a persistent nanoplasma exists within the cluster. When $\nu\lesssim\nu_p$, $\tau_{C\ell}>\tau_\ell$, the electron removal from the cluster via outer ionization is hampered, with a long lived nanoplasma being expected to prevail. The introduction of the laser frequency dependence of the electron and nuclear dynamics provides a new dimension in the exploration of outer ionization and Coulomb explosion.

## VIII. DISCUSSION

The energetics of Coulomb explosion of multicharged clusters produced by extreme multielectron ionization in ultraintense laser fields transcends the CVI approximation. The present study addresses some important aspects of Coulomb explosion of multicharged clusters. First, the effects of electron dynamics on the nuclear dynamics is manifested by the interrelation between outer ionization dynamics, Coulomb explosion energetics, and angular distribution. These effects established the features of laser intensity on the nuclear energies. Second, the effects of the laser pulse shape on the energetics of Coulomb explosion revealed quantitative characteristics of electron and nuclear dynamics in the coupled laser-cluster system.

Some novel implications of the interplay between electron outer ionization and nuclear dynamics, and of the laser-electron-nuclei coupling, emerged from our analysis. For a rectangular laser pulse shape, which provides insight into the applicability of the CVI approximation, the CVI picture prevails when complete outer ionization is attained, i.e., $t_{\mathrm{oi}}\leqslant\tau$, and when outer ionization is faster than nuclear dynamics, i.e., $t_{\mathrm{oi}}\leqslant\tau_v$, Eq. (19). The most important features of the laser pulse shape effects pertain to the realistic and physically reliable case of a Gaussian pulse, where the pseudo-CVI regime is realized over a well-characterized cluster size and laser intensity region. The characterization of the IIAFLS mechanism for high intensity ($I=10^{17}-10^{20}\,\mathrm{W\,cm^{-2}}$) Gaussian-shaped laser pulses reveals that even in this high intensity domain the CVI picture requires some extension and modification. These are manifested by the finite cluster size domain for the near applicability of the CVI energetics and in the anisotropy of the $D^+$ ions angular distribution, velocities, and kinetic energies in Coulomb explosion. The introduction of the boundary cluster radius $(R_0)_I$ and the corresponding Coulomb explosion energy $(E_{\mathrm{av}})_I$ characterizes the upper limits for the applicability range of the cluster size dependence $E_{\mathrm{av}}\propto R_0^2$ of the energetics of Coulomb explosion in the range $R_0<(R_0)_I$. The breakdown of the quadratic size equation for the energetics is manifested by a weaker cluster size dependence. From the practical point of view our analysis of the pseudo-CVI domain for Gaussian pulses establishes the applicability range and the maximal cluster size for the pseudo-CVI energetic size equation. For a given $(D)_n$ cluster size $R_0$, the optimal laser intensity $I$ of a Gaussian pulse to be used corresponds to $R_0\sim(R_0)_I$. Such optimization of the laser intensity will preclude energy disposal to electrons and maximize the energetics of Coulomb explosion for this cluster size. Finally, we would like to point out that from the point of view of future developments, pulse shaping in Coulomb explosion, which utilizes the complete picture for laser-electron-nuclear dynamics, will be of interest for the control of Coulomb explosion of molecular clusters. While the issue of pulse shaping[46,47] of ultraintense femtosecond pulses is fraught with experimental difficulties, progress has recently been made for pulse shaping in the intensity range of $I=10^{14}-10^{15}\,\mathrm{W\,cm^{-2}}$.[45]

The foregoing analysis of the energetics of Coulomb explosion of multicharged clusters provides the conceptual basis for $dd$ (and $dt$) nuclear fusion driven by Coulomb explosion of deuterium (or tritium) containing homonuclear $(D_2)_{n/2}$ [or $(T_2)_{n/2}$] clusters,[25–28,30] as well as heteronuclear[27–30,33,38] molecular clusters. The optimization of the reaction yield for these nuclear fusion reactions requires the maximization of the energetics of the $D^+$ (or $T^+$) ionic fragments for realistic laser intensities. This physical situation can be realized for Gaussian pulses in the pseudo-CVI regime. Our analysis for $(D_2)_{n/2}$ clusters (Fig. 8) reveals that for $I=10^{19}\,\mathrm{W\,cm^{-2}}$ the $E_{\mathrm{av}}\propto R_0^2$ scaling law applies for $R_0<(R_0)_I=600\,\text{Å}$ for which $(E_{\mathrm{av}})_I=700\,\mathrm{keV}$. According to our previous calculations[32] the neutron yield $Y$ per laser pulse from $dd$ fusion driven by Coulomb explosion of such $(D)_n$ clusters, under the experimental conditions of the Laurence Livermore Laboratory experiment,[25,26] is expected to be $Y\simeq 10^6$. Finally, we note the dramatic enhancement of the $D^+$ ion energies and nuclear fusion yields driven by Coulomb explosion of molecular heteroclusters of deuterium bound to heavier atoms[27–30,32] proposed by us. This will be discussed in the subsequent paper (Paper IV) in this series.[42]

## ACKNOWLEDGMENT

This research was supported in part by the Binational German-Israeli James Franck Program on Laser-Matter Interactions.

[1] R. A. Snavely *et al.*, Phys. Rev. Lett. **85**, 2945 (2000).
[2] C. Gaha, G. D. Tsakiris, G. Pretzler, K. J. Witte, C. Delfin, C.-G. Wahl-

ström, and D. Habs, Appl. Phys. Lett. **77**, 2662 (2000); U. Andiel, K. Eidmann, K. Witte, I. Uschmann, and E. Förster, *ibid.* **80**, 198 (2002).
[3] R. Storian, A. Rosenfeld, D. Ashkenasi, I. V. Hertel, N. M. Bulgakova, and E. B. Campbell, Phys. Rev. Lett. **88**, 097603 (2002).
[4] K. Boyer, T. S. Luk, J. C. Solem, and C. K. Rhodes, Phys. Rev. A **39**, 1186 (1989).
[5] J. Purnell, E. M. Sayder, S. Wei, and A. W. Castleman, Jr., Chem. Phys. Lett. **229**, 333 (1994).
[6] T. Ditmire, J. W. G. Tisch, E. Springate, M. B. Mason, N. Hay, R. A. Smith, J. Marangos, and M. H. R. Hutchinson, Nature (London) **386**, 54 (1997).
[7] T. Ditmire, E. Springate, J. W. G. Tisch, Y. L. Shao, M. B. Mason, N. Hay, J. P. Marangos, and M. H. R. Hutchinson, Phys. Rev. A **57**, 369 (1998).
[8] J. V. Ford, O. Zhong, L. Poth, and A. W. Castleman, Jr., J. Chem. Phys. **110**, 6257 (1999).
[9] M. Lezius, V. Blanchet, D. M. Rayner, D. M. Villeneuve, A. Stolov, and M. Yu. Ivanov, Phys. Rev. Lett. **86**, 51 (2001).
[10] E. Springate, N. Hay, J. W. G. Tisch, M. B. Mason, T. Ditmire, M. H. R. Hutchinson, and J. P. Marangos, Phys. Rev. A **61**, 063201 (2000).
[11] D. A. Card, E. S. Wisniewski, D. E. Folmer, and A. W. Castleman, Jr., J. Chem. Phys. **116**, 3554 (2002).
[12] T. Ditmire, J. W. G. Tish, E. Springate, M. B. Mason, N. Hay, J. P. Marangos, and M. H. R. Hutchinson, Phys. Rev. Lett. **78**, 2732 (1997).
[13] T. Ditmire, R. A. Smith, J. W. G. Tisch, and M. H. R. Hutchinson, Phys. Rev. Lett. **78**, 3121 (1997).
[14] K. Kondo, A. B. Borisov, C. Jordan, A. McPherson, W. A. Schroeder, K. Boyer, and C. K. Rhodes, J. Phys. B **30**, 2707 (1997).
[15] M. Lezius, S. Dobosz, D. Normand, and M. Schmidt, Phys. Rev. Lett. **80**, 261 (1998).
[16] I. Last and J. Jortner, Phys. Rev. A **60**, 2215 (1999).
[17] I. Last and J. Jortner, Phys. Rev. A **62**, 013201 (2000).
[18] K. Ishikava and T. Blenski, Phys. Rev. A **62**, 063204 (2000).
[19] K. J. Mendham, N. Hay, M. B. Mason, J. W. G. Tisch, and J. P. Marangos, Phys. Rev. A **64**, 055201 (2001).
[20] C. Siedschlag and J. M. Rost, Phys. Rev. A **67**, 013404 (2003).
[21] V. Kamarappan, M. Krishnamurthy, and D. Mathur, Phys. Rev. A **67**, 043204 (2003).
[22] Y. Fukuda, K. Yamakawa, Y. Akahane, M. Aoyama, N. Inoue, H. Ueda, and Y. Kishimoto, Phys. Rev. A **67**, 061201 (2003).
[23] I. Last and J. Jortner, Z. Phys. Chem. (Munich) **217**, 975 (2003).
[24] M. Schnürer, S. Ter-Avetisyan, H. Stiel, U. Vogt, W. Radloff, M. Kalashnikov, W. Sandner, and P. V. Nickles, Eur. Phys. J. D **14**, 331 (2001); S. Ter-Avetisyan, U. Vogt, H. Stiel, M. Schnürer, I. Will, and P. V. Nickles, J. Appl. Phys. **94**, 1 (2003).
[25] J. Zweiback, R. A. Smith, T. E. Cowan, G. Hays, K. B. Wharton, V. P. Yanovsky, and T. Ditmire, Phys. Rev. Lett. **84**, 2634 (2000).
[26] J. Zweiback, T. E. Cowan, R. A. Smith, J. H. Hurtlay, R. Howell, C. A. Steinke, G. Hays, K. B. Wharton, J. K. Krane, and T. Ditmire, Phys. Rev. Lett. **85**, 3640 (2000).
[27] I. Last and J. Jortner, Phys. Rev. Lett. **87**, 033401 (2001).
[28] I. Last and J. Jortner, Phys. Rev. A **64**, 063201 (2001).
[29] J. Jortner and I. Last, ChemPhysChem **3**, 845 (2002).
[30] R. W. Madison, P. K. Patel, M. Allen, D. Price, R. Fitzpatrick, and T. Ditmire, Phys. Plasmas **11**, 1 (2004).
[31] V. Kumarappan, M. Krishnamurthy, and D. Mathur, Phys. Rev. A **67**, 063207 (2003).
[32] I. Last and J. Jortner, J. Phys. Chem. A **106**, 10877 (2002).
[33] G. Grillon, Ph. Balcou, J.-P. Chambaret *et al.*, Phys. Rev. Lett. **89**, 065005 (2002).
[34] T. Ditmire, Phys. Rev. A **57**, R4094 (1998).
[35] V. P. Krainov and M. B. Smirnov, Phys. Rep. **370**, 237 (2002).
[36] I. Last and J. Jortner, J. Chem. Phys. **120**, 1336 (2004).
[37] I. Last and J. Jortner, J. Chem. Phys. **120**, 1348 (2004).
[38] I. Last, Y. Levy, and J. Jortner, Proc. Natl. Acad. Sci. U.S.A. **99**, 9107 (2002).
[39] U. Näher, S. Bjornholm, S. Fraundorf, F. Gracias, and C. Guet, Phys. Rep. **285**, 245 (1997).
[40] I. Last, I. Schek, and J. Jortner, J. Chem. Phys. **107**, 6685 (1997).
[41] Ch. Siedschlag and J. M. Rost, Phys. Rev. A **67**, 013404 (2003).
[42] I. Last and J. Jortner, *Electron and Nuclear Dynamics of Molecular Clusters in Ultraintense Laser Fields. IV. Coulomb Explosion of Multicharged Elemental Clusters and Heteroclusters* (unpublished).
[43] G. A. Mourou, C. P. J. Barty, and M. D. Perry, Phys. Today **51**, 22 (1998).
[44] M. H. R. Hutchinson, T. Ditmire, E. Springate, J. W. G. Tisch, Y. L. Shao, M. B. Mason, N. Hay, and J. P. Marangos, Philos. Trans. R. Soc. London, Ser. A **356**, 297 (1998).
[45] M. J. J. Vrakking, Eur. Phys. J. D **26**, 111 (2003).
[46] H. Rabitz, R. De Vivie-Riedler, M. Motakus, and K. Kompa, Science **288**, 824 (2000).
[47] T. Brixner, M. H. Domraus, P. Niklaus, and R. G. Gerber, Nature (London) **414**, 57 (2001).
[48] K. A. Smith, T. Ditmire, and J. W. G. Tisch, Rev. Sci. Instrum. **69**, 3798 (1998).
[49] F. Dorchies, F. Blasco, T. Caillaud, J. Stevefelt, C. Stenz, A. S. Boldarev, and V. A. Gasilov, Phys. Rev. A **68**, 023201 (2003).